CFD Analysis in Control of Urea Injection for an Automotive SCR Application

A thesis submitted in partial fulfilment of the requirement for the award of the degree of

Master of Engineering

in

Thermal Engineering

Submitted by

Himanshu Gupta
Registration No. 801783007

Under the Supervision of

Dr. Rohit Kumar Singla
(Assistant Professor, Mechanical Engineering Department)

&

Mr. Ravindra S. Deshmukh
(General Manager, Vehicle Integration (MHCV), ERC, Tata Motors Ltd., Pune)

Department of Mechanical Engineering
Thapar Institute of Engineering & Technology, Patiala, Punjab
(Deemed to be University)

July, 2019

Certification

This is to certify that the work down in this thesis title **"CFD Analysis in Control of Urea Injection for an Automotive SCR Application"** submitted in partial fulfillment of requirement for the award of Master of Engineering Degree in Thermal Engineering in the Mechanical Engineering Department of Thapar Institute of Engineering & Technology, Patiala, is an authentic record of work carried out by me under the guidance of **Dr. Rohit Kumar Singla,** Assistant Professor, Mechanical Engineering Department, Thapar Institute of Engineering & Technology, Patiala, and **Mr. Ravindra S. Deshmukh,** General Manager, Vehicle Integration, M&HCV, ERC, Tata Motors Ltd., Pune. The matter embodied in this report has not been submitted in any part or full to any university or institute for the award of any degree.

Date: 15/07/2019

Himanshu Gupta
Roll No. 801783007

This is to certify that above declaration made by the student concerned is correct to the best of my knowledge & belief.

Date: 15/07/2019

Ravindra S. Deshmukh
General Manager, VIG-MHCV,
ERC, Tata Motors Ltd.,
Pune, Maharashtra.

Date: 15/07/2019

Dr. Rohit Kumar Singla
Assistant Professor,
Mechanical Engineering Department,
Thapar Institute of Engineering & Technology, Patiala, Punjab.

Certification

This is to certify that the work down in this thesis title **"CFD Analysis in Control of Urea Injection for an Automotive SCR Application"** submitted in partial fulfillment of requirement for the award of Master of Engineering Degree in Thermal Engineering in the Mechanical Engineering Department of Thapar Institute of Engineering & Technology, is an authentic record of work carried out by me under the guidance of **Dr. Rohit Kumar Singla,** Assistant Professor, Mechanical Engineering Department, Thapar Institute of Engineering & Technology, Patiala, and **Mr. Ravindra S. Deshmukh,** General Manager, Vehicle Integration, MHCV, ERC, Tata Motors Ltd., Pune. The matter embodied in this report has not been submitted in any part or full to any university or institute for the award of any degree.

Date: 02/07/2019

Himanshu Gupta
Roll No. 801783007

This is to certify that above declaration made by the student concerned is correct to the best of my knowledge & belief.

Date: 2/07/2019

Ravindra S. Deshmukh
General Manager, VIG-MHCV,
ERC, Tata Motors Ltd.,
Pune, Maharashtra.

Date: /07/2019

Dr. Rohit Kumar Singla
Assistant Professor, MED,
T.I.E.T., Patiala, Punjab.

Acknowledgement

I would like to specially acknowledge and extent my heartfelt gratitude to all those who have helped me in completion of this thesis.

I would especially like to thank **Mr. Ravindra S. Deshmukh,** General Manager, Vehicle Integration-M&HCV, Engineering Research Center, Tata Motors Ltd., **Dr. Rohit Kumar Singla,** Assistant Professor, Mechanical Engineering Department, Thapar Institute of Engineering &Technology, Patiala, for their full support and guidance.

Furthermore, I am grateful to our team of Vehicle Integration M&HCV, Tata Motors Ltd. for their support at every step. I would also like to thank my parents for their years of love, support and encouragement in every step of my life. They have always wanted the best for me and I admire their determination and sacrifice. Besides, I would like to acknowledge my institute i.e**. Thapar Institute of Engineering & Technology.**

ERC, Tata Motors Ltd. Pune is gratefully acknowledged for providing the best platform for research.

Last but not the least; I would like to thank the God for all their good benevolence.

Date: 2/07/2019

Himanshu Gupta
M.E. (Thermal)
(801783007)

Dedicated to
Beloved Family

Abstract

Selective Catalytic Reduction (SCR) has proven to be the front runner for the removal of nitrogen oxides (NO_X) from exhaust gas. BS-VI emission regulations present a challenge from the control point of view, so as to achieve high NOx conversion while keeping the ammonia slip under control.

This thesis mainly focus upon finding the internal mechanism occurred inside the SCR. The behaviour of urea-droplet inside the SCR are investigated through CFD Ansys Simulations. The flow uniformity , temperature dependency of deposits, evaporation tendency of the mixture near the substrate are also found.

The effect of insulation of convertor cone, mass flow rate of exhaust and inlet cone length, turbulent and swirling flow, effect of different geometries in injection system, effect of different temperature ranges are further studied.

Various simulations are also performed in both transient and steady states in order to find the injectors and sprays directions, the deposits at wall formation, and evaporation tendency are also investigated.

With the help of above results we can predict the parameters such as reqiured mass flow rate of emissions, position of injection of urea spray, time for the spray etc, that can optimize the Exhaust system and provides less harmful atmosphere.

These results are validated experimentally by the exhaust system suppliers for heavy commercial vehicles.

Table of Contents

List of Table

List of Figures

Nomenclature

ANR	:	Ammonia NOx Ratio
ASC	:	Ammonia Slip Catalyst
ARAI	:	Automotive Research Association of India
BS	:	Bharat Stage
OEM	:	Original Equipment Manufacturers
CFD	:	Computational Fluid Dynamics
CPSI	:	Cells per square inch (Cells Density)
CO	:	Carbon Monoxide
DEF	:	Diesel Exhaust Fluid
DOC	:	Diesel Oxidation Catalyst
DPF	:	Diesel Particulate Filter
EATS	:	Exhaust After-treatment System
ECM	:	Engine Control Module
EGR	:	Exhaust Gas Recirculation
HC	:	Hydrocarbons
LNT	:	Lean NOx Trap
NH_3	:	Ammonia
NOx	:	Nitrogen oxides
PM	:	Particulate Matter
RM	:	Rapid Modelling
SCR	:	Selective Catalytic Reduction
UL	:	Urea Lines
UWS	:	Urea Water Solution

Mathematical Symbols

x	=	position
t	=	time
v	=	velocity
m	=	mass
F_d	=	drag force
C_d	=	drag coefficient
Re	=	Reynold's number
D	=	diameter
T	=	temperature
N	=	number of cells
c_p	=	specific heat constant
EG	=	specific heat constants for exhaust gases
S	=	specific heat constant for substrate
Sh	=	Sherwood number
B_M	=	mass transfer number
B_T	=	heat transfer number
Nu	=	Nusselt number
Pr	=	Prandtl number
Q	=	heat transfer
ΔP	=	change in pressure
U	=	velocity at various data points
U_{avg}	=	area averaged velocity
A_0	=	area of the sectional plane
D_{ev}	=	velocity deviation index
C	=	mass concentration

Greek Symbols

ρ	=	density
τ	=	time constant
γ	=	specific heat ratio
σ_{SB}	=	Stefan Boltzmann constant
ε	=	emissivity

Subscripts

d	=	droplets
exh.gas	=	exhaust gases
SCR	=	selective catalytic reduction
s	=	substrate
i	=	internal
e	=	external
wall	=	wall
SB	=	Stefan Boltzmann

CHAPTER 1
INTRODUCTION

All over the world, the automobiles exhaust emissions contributes expressively to the air pollution. In order to provide less harmful oxygen to the humankind, there is a need to implement some new methods in the vehicle emissions that releases less toxic substance such as CO, NOx and Particulate matters in the atmosphere. That is why Central Pollution Control Board, Govt. of India brought new norms to the Automobile Industries in order to achieve the above mentioned. Due to this reason, Indian Auto OEM's have to implement latest BS-VI Standards from April-2020, for providing cleaner atmosphere in India.

Bharat Stage (BS) emissions standards are the standards set up by the Govt. of India in order to regulate the air pollutants coming out from internal combustion engines, including automobiles. The BS-standards came into picture from 2000, and further modified from then onwards.

The BS-VI standards are somewhat synonyms of Euro-6 standards that are followed by several developed countries throughout the world. In the following section, we will discuss about the diesel engine combustions and the exhaust emissions from the combustion.

1.1 Diesel Engine Combustions and Exhaust Emissions

Due to the reason that diesel engines have higher thermal efficiency and lower emissions of CO, the usage of diesel engines are increasing day-by-day. But due to this, there is an increase in emissions that declines the air quality, amongst which NOx is the major pollutant.
Diesel fuel consists of hydrocarbons of higher energy densities such as $C_{10}H_{24}$ (carbon-hydrogen ratio of 1 to 2, or more) [1].

In ideal conditions, when these hydrocarbons gets combusted, it releases exhaust that consists primarily of carbon-dioxide, water and unused air. But in non-ideal conditions, various other pollutants are also produced along with CO_2 & H_2O. Common pollutants formed are namely carbon-monoxides (CO), nitrogen oxides (NOx), unburnt hydrocarbons (HC), and particulate matter (PM). NOx consists of both NO and NO_2.

The major difference in **BS-IV** and **BS-VI** emissions is in the quantity of sulphur present in the fuel. The BS-VI fuel is likely to bring a reduction of around 80% in the content of sulphur from

50 parts per million (ppm) to 10 ppm. And also the NOx emissions from diesel vehicles are likely to come down by nearly 70%.

For Heavy Commercial Vehicles, the **latest standards for Exhaust Emissions** (Source ARAI) are shown in Table 1.1:

Table 1. 1 Comparison of Emission Standards (Source ARAI)

Emission Stage	**CO (g/kWh)**	**HC (g/kWh)**	**NOx (g/kWh)**	**PM Mass (g/kWh)**	**PM Number (number/kWh)**
BS III	5.45	0.78	5.0	0.1	NA
BS IV	4.0	0.46	3.5	0.02	NA
BS VI	4.0	0.13	0.46	0.01	$6.0X10^{11}$
% Change	0	72	87	50	NA

In the following section, we are discussing about the harmful effects of NOx on the environment and the human beings.

1.2 Effects of harmful emissions on human beings

1. **CO emissions:** long term exposure can prevents oxygen transfer and increases headaches/nausea.
2. **HC emissions:** short time exposure can cause headaches, vomiting and disorientations.
3. **PM emissions:** can harm the respiratory tract and reduce lungs functioning.
4. **NOx emissions**
    - **Health hazardous effects:** NO is an irritant and is poisonous, and causes headache and nausea. Long term exposure may cause nose and eye irritation and damage lung tissues, suffocation & Cyanosis. NO is an irritant and is toxic, and can cause pulmonary enema [2].
    - **Environmental hazardous effects:** NOx in the presence of sunlight and organic compounds, reacts to form Ozone. NOx combines with H_2O and forms nitric acid and causes acid rain [3].

1.3 NOx Formation

The NOx is undesirable by-product in the Exhaust Emissions produced by the Combustion in the diesel engines due to non-ideal conditions.

The **primary sources of NOx** formation in Combustion are:

1. Thermal NOx, 2. Fuel NOx, 3. Prompt NOx

In I.C. Engines, **thermal NOx** is formed abundantly during Combustion.

Chemically, **Zel'dovich mechanism** describes the oxidation of Nitrogen and NOx formation. At high temperatures, the rate of formation of NO increases and the equilibrium state is reached with time. But as the temperature drops sharply during the expansion stroke, large amount of NOx formed at high temperatures does not reaches equilibrium. Such state is called frozen state.

When nitrogen compounds reacts with the oxygen, **Fuel NOx** are formed.

In the early stages of combustion, as the hydrocarbons reacts with nitrogen, intermediates for e.g. HCN &H_2CN gets formed. From this **Prompt NOx** are formed, and later gets oxidises to NO.

1.3.1 Non Commercial methods for NOx Reduction

Non-Commercially following techniques are helpful in the reduction of NOx:

a) **Lean NOx catalysts**

In Lean NOx catalysis, when exhaust gases are passing from the silencer some hydrocarbons are added to them, that reduces NOx and forms N_2, CO_2 and H_2O. This technique reduces relatively very less amount of NOx only 15% - 20%. Therefore, this technique is becoming obsolete.

b) **NOx adsorbers**

NOx adsorbers are used simultaneously together with the Lean NOx Catalyst. This combination adsorbs the NOx, which are released at temperatures which are favourable for the reaction with hydrocarbons [3].

These NOx adsorbers also adsorbs the sulphur which causes irreversible deactivation of the catalyst and makes sulphur poisoning, hence are not used in diesel engines [1].

c) **Plasma-assisted catalyst**

In plasma assisted catalysis, in order to oxidize and reduce the NO molecules, a non-thermal plasma is used because it generates radicals and these radicals can reduces NO molecules. With the oxygen which exist in the exhaust emissions, NO gets oxidized to NO_2, lowering the NOx reduction. This technique requires some more development for commercial use.

This upgradation from BS-IV to BS-VI in order to reduce the NOx emissions, causes design changes in different aggregates for a vehicle, such as the Engine, the Air Intake System consisting of Radiator, Intercooler, Turbocharger and the Exhaust System.

From the various literatures, we come to kow that the Exhaust system in heavy commercial vehicles is most affected in terms of number of changes. Thus, we consider the changes and carry forward our research in this area. The need of meeting these rigorous requirements with respect to NOx emissions has led to the advancements of several after-treatment techniques.

In further chapters we will study the exhaust system of a vehicle and the various after-treatment techniques used for saving the environment.

CHAPTER 2

TECHNICAL BACKGROUND

2.1 System Architecture of Exhaust System

The system architecture of the exhaust system, with the pattern of flow is shown in figure 2.1.

In many trucks/lorries all or most of the exhaust system is visible, often with a vertical exhaust pipe. Often in such trucks the silencer is surrounded by a perforated metal sheath to avoid people getting burnt touching the hot silencer. This sheath may be chrome plated as a display feature. Part of the pipe between the engine and the silencer is often flexible metal industrial ducting, which helps to avoid vibration from the engine being transferred into the exhaust system. Sometimes a large diesel exhaust pipe is vertical, to blow the hot noxious gas well away from people; in such cases the end of the exhaust pipe often has a hinged metal flap to stop debris, birds and rainwater from falling inside.

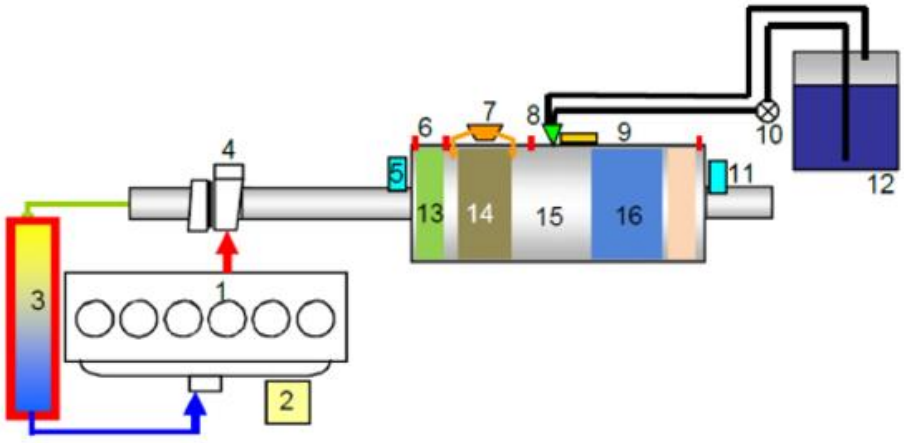

Figure 2. 1 System Architecture of the Exhaust System

1. Engine
2. ECM (Engine Control Module)
3. Charge Air Cooler
4. Turbocharger
5. Engine Out NOx Sensor
6. Temperature Sensor (x4)
7. ΔP Sensor
8. UL_3 Dosing Module
9. Sensor Table
10. UL_3 Supply Module
11. System Out NOx Sensor
12. DEF Tank
13. DOC Catalyst
14. DPF
15. Mixer
16. SCR Catalyst

2.2 After Treatment Techniques for NOx Reduction from Exhaust System

After treatment techniques are used to reduce NOx, which is non-controllable compound rises from fuel composition & combustion phenomenon. In order to reduce the toxic gases, following After-treatment techniques are used and are under research & development for the Exhaust System:

1. Exhaust Gas Recirculation (E.G.R.),
2. Diesel Particulate Filter (D.P.F.),
3. ReGen,
4. Lean NOx trap (L.N.T),
5. Selective Catalytic Reduction (S.C.R.),
6. Diesel Oxidation Catalyst (D.O.C.),
7. Ammonia Slip Catalyst (A.S.C.).

Urea-SCR is an evident and proven technique. With the help of reductant ammonia, it produces conversion efficiency of about 96-99%.

2.2.1 Exhaust Gas Recirculation

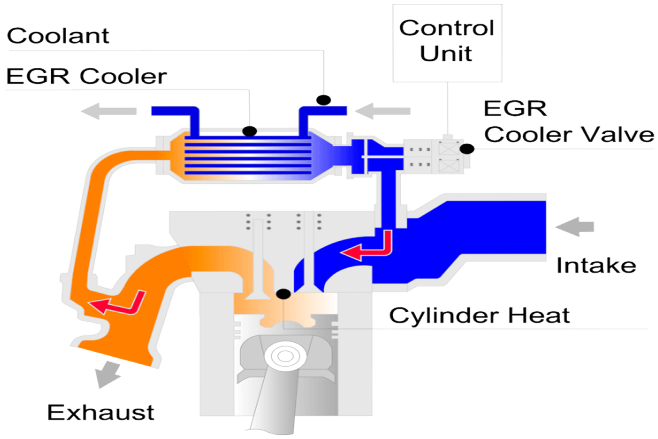

Figure 2. 2 EGR System [4]

EGR recirculates some portion of exhaust gases back to the engine cylinders as shown in figure 2.2. This process dilutes the oxygen and provides combustion gases to work as an absorbent to reduce the topmost in-cylinder temperatures. NOx are generally produced at high temperatures and at maximum pressure.

For diesel engines, the gases in the EGR are cooled with heat exchangers in order to have larger mass of recirculated gases. As diesel engines always works with excess of air, hence EGR rates

in NOx Control are found to be near about 50%. Exhaust gases recirculated back to the engine cylinders increases the wear rate as the carbon particulates in the exhaust gases degrades the rings and the cylinder walls [5].

When the diesel engine is not throttled, the EGR does not lower down the throttling losses. During the power stroke, EGR declines the specific heat ratio of the combustion gases and the amount of fuel burnt. This increases the PM emissions that further increases the EGR [6, 7].

As the PM does not gets burnt during the power stroke, so we need to compensate these PM increment in the EGR. This can be done by using Diesel Particulate Filter (DPF). DPF cleans the exhaust but due to the creation of back pressure it causes a marginal reduction in fuel efficiency.

During the operating conditions, NO_2 is the primary oxidizer of soot trapped in the DPF. This process is called as Passive Regeneration. As the rate of EGR increase, there is a reduction in the efficiency of passive regeneration in particulate filter. So, there is a requirement in active regeneration of DPF at smaller intervals. This can be attained by burning the diesel in presence of oxidation catalyst, this increases exhaust gas temperature over the DPF, where PM is burnt by remaining oxygen present in the exhaust.

By providing lower oxygen content exhaust gas to the intake, EGR lowers down the combustion temperature, thus reduces NOx emissions. This will declines the combustion efficiency and hence compromise the engine power and fuel economy.

EGR causes issues like swirl flaps with the fitted components. With the starting of DPF, the soot production rate in the EGR increases. Also, due to addition of abrasive impurities and increment of acidity of engine oil, the EGR systems reduces engine durability [8, 9].

There are two methods used in injection of the fuel:

a) straight into the engine cylinders during the exhaust stroke,

b) downstream injection directly into the exhaust stream/ downstream of the turbo.

2.2.2 Diesel Particulate Filter (DPF):

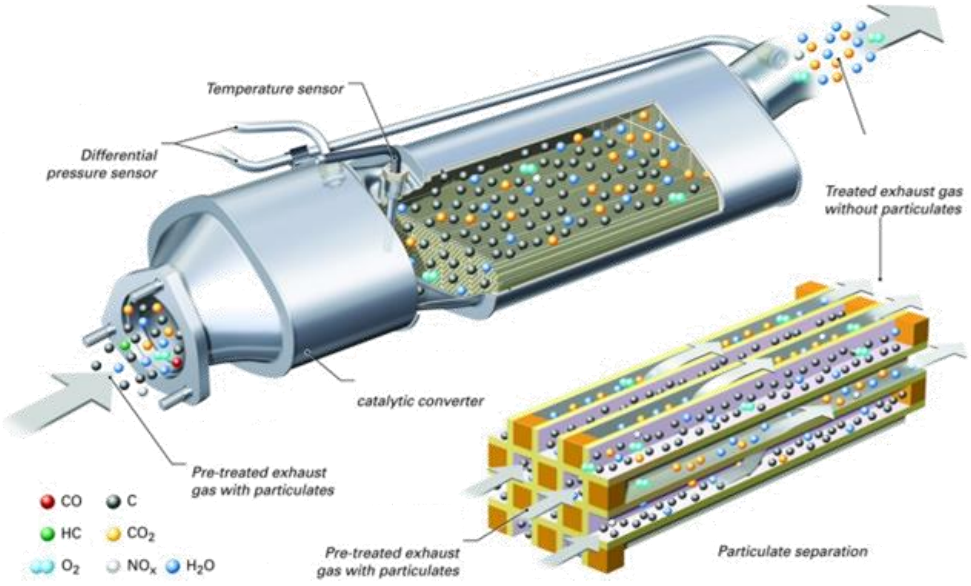

Figure 2. 3 Diesel Particulate filter in SCR [10].

Diesel Particulate filter became the most effective method to remove soot or diesel particulate matter from the diesel engine exhaust. It substantially capture the particulates of diesel in order to prevent their discharge in the atmosphere. Diesel particulate filter materials shows notable filtration efficiencies of more than 90%, and also they have good mechanical and thermal durability.

In diesel engines, due to the incomplete combustion, fuel air mixture generates different types of particles. These particles are known as DPM (Diesel particulate matter) that generates black carbon particles known as soot. With optimal DPF, these soot emissions can be reduced to 0.0012 g/km or less [11].

The formation of these soot particles are also influenced by the

a) Quality of fuel (e.g. high sulphur content fuel produces more particles, while low sulphur fuel produces less particles).

b) Injection pressure of fuel.

c) Inadequate position of DPF in exhaust are likely to built-up soot, which causes high back pressure and hence causes engine related issues [12].

DPF needs more maintenance than Catcon. Catcon follows a flow-through mechanism, while DPF keeps larger exhaust particles by forcing the exhaust gas through filter and flows smaller

exhaust particles through it. Maintenance-free DPF breaks the larger particles into smaller particles.

In some filters the ash that does not gets fully converted into gas and remains in solid form, and it will gets accumulated at walls of the filter, hence enhances the exhaust pressure at the face of the filter. So they can be used only once. While other filters burnt the accumulated PM passively by the use of catalyst or actively with the help of fuel burners that burns the soot at combustion temperature. Hence, regular maintenance of DPF is a necessity. Cleaning them should be done carefully in order to save the filter from damaging. Simultaneously, turbochargers and fuel injectors also needs necessitate cleaning. Wall-flow DPF have soot cleaning efficiency of 85% and above. The internal structure of DOC and DPF in after-treatment system is shown in Figure 2.4.

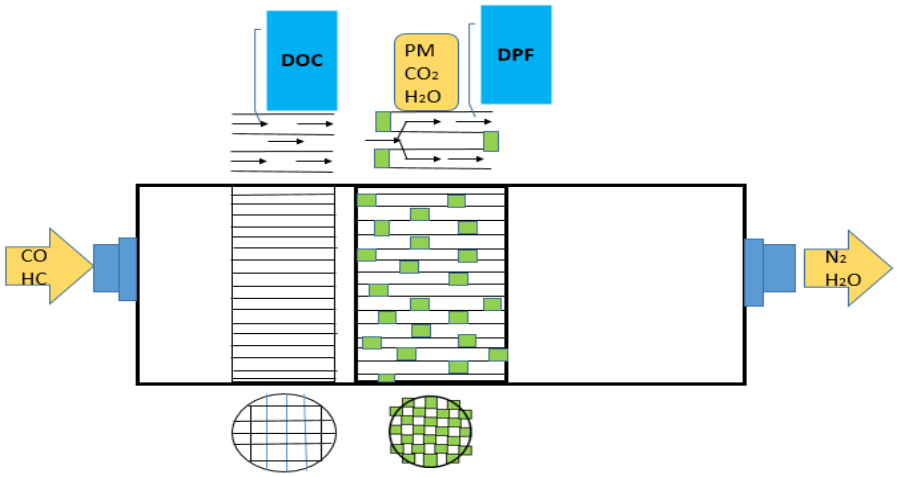

Figure 2. 4 Internal Structure of DOC & DPF in After-treatment System [13].

Types of DPF:

1. Cordierite wall flow filters
2. Silicon carbide wall flow filters
3. Ceramic fiber filter
4. Metal fiber flow-through filters
5. Paper
6. Partial filters

2.2.2.1 Collection & Regeneration

As diesel particulates have low bulk density normally under 0.1 g/cm^3, these DPF can rapidly accumulate substantial litres of soot. From an older buses or heavy-duty trucks engine, several litres of soot per day may be collected. These collected soot particulates would ultimately cause exceptionally high pressure drop of exhaust gases in the filter, and this would declines the effectiveness of the engine operations. Therefore, for restoring the soot collection capacity of the filter, the DPF systems requires a mode of removing particulates from the filter. This

method of removing of particulates, is said to be as filter ***regeneration.*** DPF passes through regeneration process which helps in removing soot and declines the filter pressure.

There are three types of regeneration processes in DPF: passive, active, and forced.

a) **Passive regeneration** occurs usually during driving, at that time engine load & vehicle drive-cycle generates temperatures which are sufficient to regenerate and build up the soot on DPF walls.

b) **Active regeneration** occurs when the vehicle is in use. At that time, the lower engine load and lower exhaust gas temperatures constrain the naturally occurring passive regeneration. The mixture of exhaust gas and fuel passes through the Diesel Oxidation Catalyst (DOC). This will creates temperatures sufficiently high to burn off the soot accumulated. As the pressure drop declines to the calculated value through the DPF, the process gets finished and begun again when there is a rebuild of soot takes place.

c) A **forced regeneration** occurs as the soot accumulation extends to a level which potentially damage the engine or the engine exhaust system, then the system requires a regeneration occurred manually with the help of a computer programming.

Thermal regeneration of DPF is normally employed, where the collected particulates are oxidized—by nitrogen dioxide and/or oxygen—to the gaseous products, primarily to carbon dioxide as shown in figure 2.5. Thermal regeneration, is definitely the cleanest and most attractive method of operating diesel particulate filters.

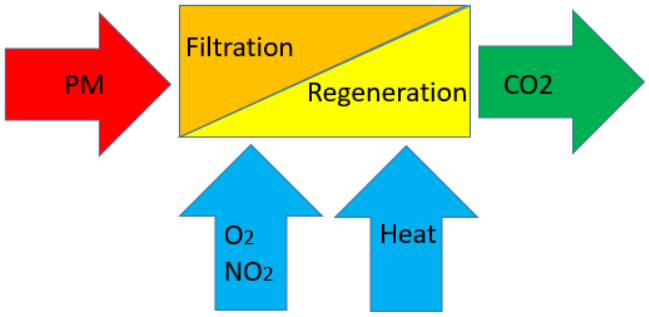

Figure 2. 5 DPF with thermal regeneration

Diesel particulate matters usually burnt at temperature above 600°C. This temperature needs to be reduced to 350°C to 450°C, by using a fuel borne catalyst. There is a further increase in temperature occurs due to starting of combustion. In certain cases, the combustion of PM raises the temperature of the filter material above the structural integrity threshold, when the fuel borne catalyst is not present. This causes an objectionable failure of the substrate material. For

limiting this possibility, several strategies were developed. As diesel engines have a high oxygen content, which makes fast regeneration of the filter, which enhance regeneration issues.

2.2.3 Diesel Oxidation Catalyst (DOC)

DOC promotes oxidation of various exhaust gases components by oxygen, which is already present in sufficient quantity in diesel exhaust. CO, HC and Organic Diesel Particulates can be oxidized to harmless products using the DOC as shown by figure 2.4. This leads to generation of Sulphur particulates and therefore, even with decline in organic fraction, it will enhance the total particulate emissions. Now-a-days, DOC is used to increase the nitrogen dioxide content of exhaust emissions, in order to support SCR catalysts & DPF performance.

When CO, HC, OF and unregulated emissions such as PAHs or aldehydes are passed over oxidation catalyst, they are oxidized to harmless products and can be controlled by the DOC. DOC oxidize NO and NO_2 gases that supports the performance of SCR catalysts and DPF used for NOx reduction [14].

The three stages that are included in catalytic oxidation reaction:

i) Oxygen is bonded at catalytic site

ii) Reactants, such as CO and HC, diffuse to the surface and reacts with the bonded oxygen.

iii) Reaction products such as CO_2 & water vapors, desorbs from catalytic sites and diffuse to the bulk of exhaust gas.

The oxidation of hydrocarbons and CO in diesel emissions can be described by the following chemical reactions:

$$Hydrocarbons + O_2 \rightarrow CO_2 + H_2O \tag{2.1}$$

$$C_pH_q + (p + \frac{q}{2}) \rightarrow pCO_2 + qH_2O \tag{2.2}$$

$$2CO + O_2 \rightarrow 2CO_2 \tag{2.3}$$

Reactions (2.1) and (2.2) represent two processes: the oxidation of gaseous phase hydrocarbons, as well as the oxidation of organic fractions of diesel particulates. Reaction (2.3) describes the oxidation of carbon monoxide to carbon dioxide. Since carbon dioxide and water vapour are considered harmless, the above reactions bring an obvious emission benefit. The oxidation of HCs also results in a reduction of the diesel odour.

Catalyst material used in DOC: Palladium (B.P.: 2963°C; M.P.: 1554.9°C)

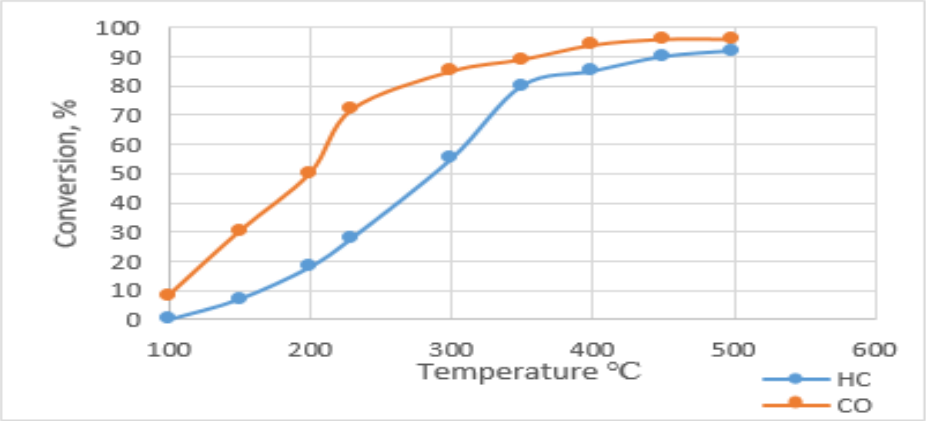

Figure 2. 6 Conversion of Hydrocarbons and Carbon-monoxide w.r.t. temperature

Diesel exhaust contains sufficient amounts of oxygen, necessary for the above reactions. The concentration of O_2 in the exhaust gases from diesel engine varies between 3 and 17%, depending on the engine load. Typical conversion efficiencies for CO and HC in the diesel catalyst are given in figure 2.6. The catalyst activity increases with temperature. A minimum exhaust temperature of about 200°C is necessary for the catalyst to "light off". At elevated temperatures, conversions depend on the catalyst size and design and can be higher than 90%. However, an oxidation catalyst will promote oxidation of all compounds of a reducing character; some of the oxidation reactions can produce undesirable products and, in effect, be counterproductive to the catalyst purpose. Oxidation of SO_2 to SO_3 with the subsequent formation of sulfuric acid (H_2SO_4), described below, is perhaps the most important of these processes.

$$2SO_2 + O_2 \rightarrow 2SO_3 \tag{2.4}$$

$$SO_3 + H_2O \rightarrow H_2SO_4 \tag{2.5}$$

When the exhaust gases are discharged from the tailpipe and mixed with air, either in the environment or in the dilution tunnel which is used for particulate matter sampling, their temperature decreases. Under such conditions the gaseous H_2SO_4 combines with water molecules and nucleates forming (liquid) particles composed of hydrated sulfuric acid. This material, called sulphate particulates, contributes to the total particulate matter emissions from the engine. Catalytic formation of sulphates, especially in conjunction with high sulphur content diesel fuel, can significantly increase the total PM emissions and, thus, become prohibitive for the catalyst application.

The oxidation of NO to NO_2 is essential for the operation of modern diesel emission control systems, where the DOC is an auxiliary catalyst supporting the performance of other types of

catalysts positioned downstream of the oxidation catalyst that require an elevated NO_2/NO ratio.

$$2NO + O_2 \rightarrow 2NO_2 \tag{2.6}$$

NO_2 usually improves the efficiency of different SCR catalysts and also enhances the passive regeneration of DPF. While DOCs are optimized for increased NO_2 in SCR.

2.2.4 Lean NOx Trap (LNT)

LNT is a device used to reduce NOx emissions coming from lean burnt fuel in IC Engine using adsorption. Lean burnt fuel in diesel engines, have higher levels of oxygen content in the exhaust gases. The LNT was designed due to the limited effectiveness of EGR and variable supply of reductant into the exhaust. Adsorbant for e.g. Zeolite traps NOx molecules and behaves like a molecular sponge. Reactants are used in order to "Regenerate" or "Purge" the trap is diesel fuel injection before the absorber regenerates it. This will made NOx to desorb and within rich conditions to react with hydrocarbons, and produce nitrogen and water.

The LNT involves storing of NOx at lean exhaust situations at the catalyst wash-coat and its discharge at rich exhaust situations or/and high temperatures.

Traps got poisoned by SOx that adsorbs more than NOx, and necessitates regeneration at high temperatures which reduces operating life of absorber [15].

2.2.5 Ammonia Slip Catalyst (ASC)

As the vehicle moves under the dynamic driving cycle, this leads to the leaving of recognizable amount of ammonia from SCR. A smart catalyst design is followed by the ASC in order to ease the additional NOx emission.

NH_3 entering into the ASC gets partially oxidized to NO. The ammonia which is inside the ASC (not yet oxidized) and the freshly oxidized NO thus reacts to N_2. The ASC is adept of eliminating the traces of Ammonia and converting in parallel newly formed and existing NO to N_2, will helps to reduce further NOx emissions.

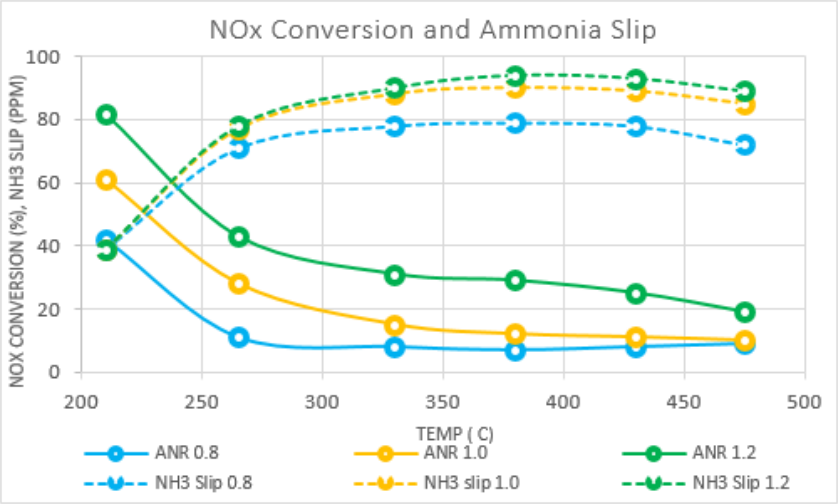

Figure 2. 7 NOx Conversion and Ammonia Slip

From the above figure 2.7, we can conclude that increase in NH_3 results into increase in NOx conversion, meanwhile also increase the NH_3 slip. Due to insufficient NH_3 and lower NH_3 slip, at 0.8 ANR, along with 1:1 stoichiometry, maximum Conversion of NOx is 85%. At 1.0 ANR, both maximum NOx conversion and NH_3 Slip are higher. At 1.2 ANR, surplus NH_3 allows even more NH_3 conversion along with higher NH_3-slip. Even the optimum catalyst, with non-uniform ammonia distribution cannot accomplish maximum NOx conversion [16].

- Reasons for non-uniform ammonia distribution:
  - i) Injection system and control system
  - ii) The Mal-distribution of flue gases.
  - iii) Fluctuating load & NOx values at inlet.
- Results of non-uniform ammonia distribution in localized ANRs:
  - i) If ANR<1: Incomplete conversion of NOx.
  - ii) If ANR>1: NH3 slip.

Ammonia Slip Catalyst:

i) Reimburses for the distribution of non-uniform ammonia.

ii) Allows operation at higher ANR. This reduces NH_3 slip and enhances NOx conversion.

iii) Improves conversion of Hydrocarbons.

iv) Provides conversion of CO formed as a result of incomplete combustion of hydrocarbons.

v) Reduces the need of oxidation catalyst.

2.2.6 Selective Catalytic Reduction

In a SCR system shown in figure 2.8, ammonia (NH_3) is used as a reducing agent to convert NOx into nitrogen gas (N_2) and water (H_2O). The main advantage with this system is the high NOx conversions (90% or higher). The disadvantages involves the space required for the catalyst, high capital- and operating costs, formation of other emissions (NH_3 slip) and formation of undesirable compounds which may lead to catalyst masking and deactivation. The NH_3 slip can be controlled by installing an oxidation catalyst after the SCR system.

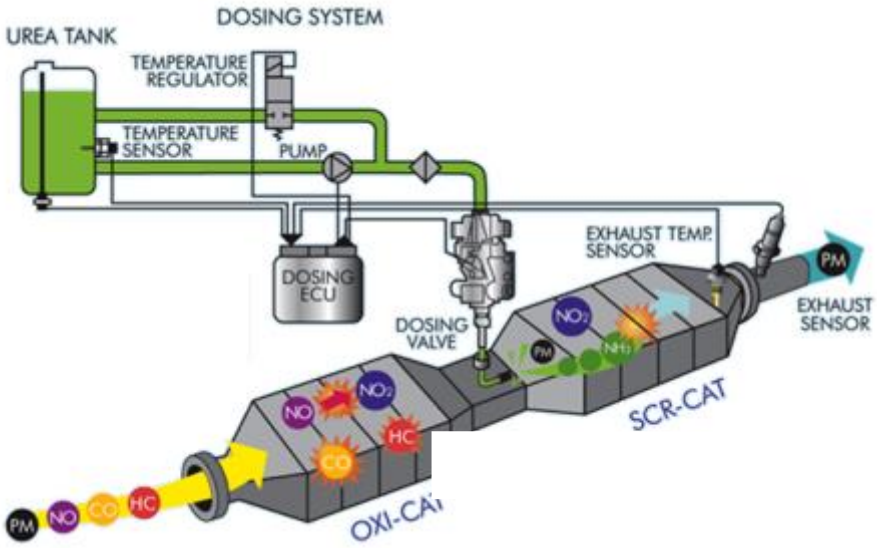

Figure 2. 8 Selective Catalytic Convertor in Exhaust System [17].

2.2.6.1 Selective Catalytic Reduction of NOx

Under the lean conditions of diesel combustion, despite of high oxygen concentration, the NOx can be reduced in the selective catalytic reduction, by using a suitable catalyst and an effective NOx reductant. Ammonia is an extensively used reductant, due to its higher sensitivity to NOx.

Ammonia can be supplied using the injection of either of aqueous or gaseous ammonia or as aqueous urea that will be converted to ammonia after injection. As ammonia is a volatile material thus due to safety reasons, injection of urea is preferred.

The stationary SCR systems have constant load which indicates the constant operating conditions irrespective of exhaust temperature and exhaust flow and there is no limitations on catalyst volume. Due to the space limitations on catalyst volume and the fluctuating engine loads, there are many challenges in obtaining the desired NOx conversions in automotive applications.

2.2.6.2 Reactions occurring in SCR catalyst

NO and NO_2 reacts selectively with NH_3 that works as a reductant in the SCR catalyst. Overall reactions occurring in the reactor are the adsorption desorption equilibrium of ammonia and the reactions between NH_3 and the NO*x* species, where NH_3 is adsorbed on a catalytic site, are expressed in equation (2.7)-(2.10) [18].

$$NH_3 \leftrightarrow NH_3 \tag{2.7}$$

$$4NO + 4NH_3 + O_2 \rightarrow 4N_2 + 6H_2O \tag{2.8}$$

$$4NO_2 + 4NH_3 \rightarrow 3.5N_2 + 6H_2O \tag{2.9}$$

$$NO + NO_2 + 2NH_3 \rightarrow 2N_2 + 3H_2O \tag{2.10}$$

The equation (2.8) is known as the standard SCR reaction generally occurs at temperatures above 200°C, the reaction rate is significantly faster for higher temperatures [19]. The equation (2.9) is known as the slow SCR reaction generally occurs at temperature below 275°C, in the presence of excess NO_2. The equation (2.10) is known as the fast SCR reaction, generally occurs at temperatures as low as 140-170°C and is favoured by an equimolar mixture of NO and NO_2 [19]. At lower temperatures and low reaction rate of the standard SCR reaction, the effect of NO_2 in the exhaust gas has higher significance at low temperatures.

From [20] and [19], we find that NO comprises of above 90% of the NO*x* in the exhaust gas, so in order to favour the fast SCR reaction, we need to make the ratio of NO/NO_2 optimal as 1:1, which favours fast SCR reaction. At lower temperatures, this can be achieved by increasing the NO_2 amount in exhaust gas. This can be done by placing an oxidation catalyst upstream the SCR catalyst. Besides this, the reaction for oxidation of NO to NO_2 occurs over iron exchanged zeolites is given in equation (2.11) [21].

$$2NO + O_2 \rightarrow 2NO_2 \tag{2.11}$$

Equation (2.12) and (2.13), shows oxidation of ammonia, which leaves less ammonia for NO*x* reduction.

$$4NH_3 + 3O_2 \rightarrow 2N_2 + 6H_2O \tag{2.12}$$

$$4NH_3 + 5O_2 \rightarrow 4NO + 6H_2O \tag{2.13}$$

The oxidation of ammonia, occurring in equation (2.12), is significant at temperatures above 400°C on Fe-Zeolite catalyst [21], while (2.13) is significant at higher temperatures above 450°C on a V-based catalyst [22]. Also, the formation of Nitrous oxide (N_2O) occurs above 450°C and the formation of Ammonium Nitrate (NH_4NO_3) occurs below 200°C [22].

2.3 Ammonia in SCR

Ammonia from urea behaves variably in different atmospheric conditions. In the following section, the whole process in SCR system is explained.

2.3.1 Ammonia as reductant

Ammonia supply can either be aqueous ammonia, gaseous ammonia, solid ammonia (Amminex's AdAmmine), or as aqueous urea (Known as AdBlue in Europe) that can be converted to ammonia in situ. Furthermore, for automotive applications aqueous urea is the choice of ammonia supply, due to safety considerations.

2.3.2 Factors that influence the SCR catalyst performance

There are several factors that influence the degree of NO*x* conversion in a SCR catalyst using ammonia as reductant:

i) Temperature
ii) Space velocity
iii) Availability of NH_3
iv) NO to NO_2 ratio

2.3.3 Ammonia formation from urea

After the injection, the aqueous urea (H_2CONH_2) gets converted to ammonia. Generally this requires three steps: i) Evaporation of water, ii) Thermal decomposition of urea, iii) hydrolysis of iso-cynaic acid.

As the urea is injected into the exhaust pipe, evaporation of water takes place inside it, where the temperature is above 100℃. The physical state of urea is unknown, in this temperature range of 100℃ to 150℃. Though it is recommended that the urea can be either molten, solid or highly aqueous solution [23, 24].

The thermal decomposition of urea begins in the temperature range between 133℃ to 160℃ and happens in the upstream of SCR catalyst, thus forms ammonia (NH_3) and iso-cynaic acid (HNCO), as stated in equation (2.14) [22,23].

$$H_2CONH_2 \rightarrow NH_3 + HNCO \tag{2.14}$$

Conversion efficiency of above reaction depends upon temperature. At temperatures above 250℃, other products such as ammeline, melamine, cyanurates and ammelide are formed [23].

Iso-cynaic acid is further hydrolysed and forms ammonia and carbon-dioxide, stated in equation (2.15)

$$HNCO + H_2O \rightarrow NH_3 + CO_2 \quad (2.15)$$

For the catalytic reaction of hydrolysis of iso-cyanic acid, nearly 50% of the NH_3 is not released upstream the SCR catalyst for gaseous phase where no substantial hydrolysis occurs at temperature below 300°C. [22, 23].

2.3.4 Ammonia coverage

The ammonia used here, is initially adsorbed on the catalyst and happens due to the strong acidic properties of the SCR catalyst surface by activity of both Bronsted and Lewis acid sites. The amount of adsorbed ammonia is referred to as the ammonia coverage.

Factors that affects the ammonia coverage are:

- Catalyst material
- Temperature
- Presence of other adsorbates

As zeolites have a higher coverage than V-based catalysts, thus material of catalyst is of great importance. A steady state ammonia storage of a zeolite catalyst can be 1.4 g/l at 200°C compared to a vanadium catalyst for which a steady state storage can be 0.4 g/l at the same temperature [22].

Also, the ammonia storage potential is highly temperature dependent. At low temperatures large amounts of ammonia can be stored, however, the ammonia storage potential is decreasing significantly with increasing temperature between 200°C and 300°C, and at temperatures above 350°C and 400°C almost no ammonia is stored in the vanadium and zeolite catalysts, respectively [22]. Thus, temperature ramps in the catalyst bed can lead to significant ammonia slip. Other compounds, for e.g. water can adsorb on the catalyst and thereby have an influence on the adsorption of NH_3.

2.4 Urea injection system

In an urea based SCR System, a solution of urea (32.5% by weight) and water, also known as AdBlue is injected into the hot exhaust gases through atomization. The water needs to evaporate before the urea decompose to NH_3 [25].

The major purpose of this injection system is to ensure proper preparation of the reductant upstream of the SCR catalyst, independent on the operating conditions. This preparation involves sufficient spatial distribution of the reductant and as high ammonia formation upstream the catalyst as possible.

Various factors that can influence the release of NH_3 are poor atomization and spatial distribution as well as deposition of solid urea in the equipment. So, proper spray properties and usage of a mixing device are important [24]. For increasing the amount of NH_3 formed upstream the SCR catalyst, a hydrolysis catalyst can be used, or the gaseous ammonia can be formed before injection [22].

2.5 Sensors used in Urea SCR System

2.5.1 Delta P Sensor

The pressure is delivered to the sensors with removable probes and rubber tubes. Measures the pressure before and after the DPF. The delta P sensor tubes are oriented correctly so that the condensation drains always maintains some distance from the sensor body. Gathers data to monitor DPF heath as well as soot and Ash loading. This data is used to trigger regens. Sensor is mounted directly on DPF sensor table. The tubes can be removed for cleaning and inspection.

2.5.2 NOx Sensor

There are 2 sensors for each system: one at engine out located near turbo outlet, while another at System outlet located at SCR outlet. These are used by ECM to calculate the NOx conversion efficiency in the primary system function. Its probe and module is non serviceable. This is non-programmable. This is a self-diagnosing and intelligent device.

After this basic introduction and a brief understanding of this whole exhaust after treatment system, we shall proceed towards the literature survey, from where we come to know the recent trend of research in this area.

CHAPTER 3

LITERATURE SURVEY

3.1 Generalised Literature Review

A lot of studies were made on the exhaust after-treatment system in a truck in multi-dimensional aspect were made in the past by several researchers. This chapter reviews different literatures published by various researchers, which put the foundations of our present work. Reviewing the different literatures provides us multi-dimensional and technical aspects about this topic, the gap findings, latest technologies used etc. which will works as a guideline for this thesis. Several researchers investigated the droplet evaporation, vaporization and the different heat transfer mechanisms [26, 28, 32, 38, 46, 48] related to the exhaust systems which proceeds in the direction of urea deposits formations and wall impingements along with static mixers [32, 39,43]. Also, few of them investigated about the flow uniformity index between urea and exhaust gases [27, 34]. Several other researches in the direction of NOx conversion efficiencies and catalyst effectiveness [30, 37, 42, 49]. Many of the researchers are investigated in the direction of compactness of exhaust system [36, 41, 44, 45, 50]. And many of them investigated the behaviour of droplet in injected spray [29, 33, 35, 40]. Thus, the literature provides us multi-dimensional and broad aspects to perform our research work.

3.2 Literature Summary

Abramzon B., *et. al.*, (1989), [26], re-examined the droplet vaporization model used in spray combustion modelling calculations in order to develop a new model of heat transfer within moving circulating droplet. The model includes variable physical properties and Lewis no. non unitary which influence the blowing (Stefan's law) on HMT and effect of transient liquid heating inside the internally circulating droplet. This incorporate the Stefan flow on the thickness of thermal diffusional films. The model simultaneously traces the life history of individual droplets.

Alekhya R., *et. al.*, (2017), [27], simulates conjugate heat transfer on the exhaust after-treatment system (EATS) for determining heat transfer to the surroundings, temperature & pressure drop in the exhaust gases, flow uniformity index and flow field at the inlet of Cat-Cons. They found that EATS box ensures a better thermal management. This EATS with thicker box insulation in comparison with thinner insulation, leads to lower heat transfer to the

surroundings, lower surface temperature and higher exhaust gas temperature. This also leads to design modularity in the exhaust system of the vehicle.

Birkhold F., *et. al.*, (2007), [28], investigated the evaporation of water from a single droplet of UWS theoretically by a Diffusion Limit model and a Rapid Mixing model, which considers variable properties and droplet motion of the solution. Rapid Mixing model is implemented in CFD and is extended to describe the urea thermal decomposition after the evaporation of water. Therein, the Lagrangian particle tracking is treated for UWS droplets. The evaporation model is extended for thermal decomposition and droplet boiling of urea. Various CFD simulations of a SCR DeNOx-system used to determine the kinetic parameters of the urea decomposition such as urea concentration and temperature of UWS droplets and urea particles.

Damm M.A., (2017), ***et. al.*,** [29] uses a new mixing element with structured porous ceramic for the homogenization and evaporation of the urea solution, that usually done by metallic mixing elements. The mixing element is used for optimizing the system with an enlarged surface with a special catalytic coating of basic polyurethane foams for attaining high NH_3 conversion rate along with the adjustable backpressure. The optimised flow dynamics of the exhaust gas and the additional special catalytic coating lead to a high-performance mixing element.

Dio C., *et. al.*, (2018), [30], investigated the factors affecting the NOx conversion efficiency using engine bench testing. They found that the older SCR deNOx system was improved by the combined catalytic oxidation device. They also studied the effect of increased urea injection on NOx conversion efficiency and the influence of NH_3 at different rpms and torques of the engine. The conversion efficiency of NOx can reach from 79.1% to 99.9%. There are issues in SCR open loop control for steady state reducing agent dosage and agent control strategy, permitting the transient conditions to the dynamic distribution of engine exhaust back pressure.

Dixit M., *et. al.*, (2016), [31], uses Gem-3D and GT-POWER tool for pre-processing and resonator modelling and simulation of muffler for finding back-pressure in the exhaust system. They considered different shell & pipe discretization element shapes & sizes for their work. They also perform the analysis of discretization factors on cold & exhaust systems. They found that the pipe discretization length along with resonator and muffler shell discretization in the three dimensions is the major contributors in finding the back pressure at a very early stage for choosing optimized design of the exhaust system of heavy commercial vehicle.

Hüthwohl G., *et. al.*, (2011), [32], evaluates the influence of the spray quality on AdBlue evaporation and the decomposition of urea droplets and performance of catalyst by using nozzle and air supply strategy dosing. They found that by electrical air supplying to the air assisted system, we have a good mixing characteristics and small nozzle of airless systems and these are provided without having the effort of air supply.

Jeong S.J., *et. al.*, (2003), [33], studied the best possible monolith combination of auto catalyst for warm-up reference and improving flow uniformity, and find combined variable cell density is effective in flow uniformity improvement & reduction of pressure drop in comparison to conventional uniform cell density. They also found that the flow distribution hugely affects the residence time, temperature, flow distribution and concentration in designing of the auto catalyst. Combined monolith in SCR showed weaker thermal resistance when compared to a conventional one. Thus, in underfloor condition and under closed coupled condition ensures better fluid dynamic performance.

Jeong S.J., *et. al.*, (2005), [34], performed a 3-D thermo-fluid analysis for a 2-Phase flow using Eulerian-Lagrangian formulation in order to achieve best design for urea SCR system in Truck. They find that with the increase in the distance between injector tip and monolith face, the uniformity increases. Also, 4-hole injector system gives best ammonia uniformity within SCR monolith for different injector locations and injection pressures in Urea-SCR and reduces the NH_3 slip and improves the performance of NOx conversion.

Kim T., *et. al.*, (2017), [35], examine the performances of various heat spreader along with, positive temperature coefficient (PTC) designs according to temperature distribution, liquid fraction, and phase-interface velocity under input condition. The heat spreader have optimal shape like turbine blades which is required to prepare adequate amount of molten UWS for normal de-NOx performance of urea SCR system.

Konstandopoulos A.G., *et. al.*, (2015), [36], studied the impact of DPF, EGR & SCR devices on fuel consumptions, pollutant emissions and urea consumption. They performed 1-D & 3-D CFD tools using GT-Power & KIVA 4-D to provide accurate predictions of exhaust emissions.

Michelin J., *et. al.*, (2015), [37], finds that the catalytic products permits the SCR active compounds to move from the ceramic substrate, which is located in the underbody to the DPF substrate already located in a close coupled position to achieve the benefit of the highest temperature. They proposed an appropriate "V-shape" of angle about 135˚ in between the DOC inlet and the SCR-coated DPF outlet for a transversal engine installation. They found that the

new mixing concepts related to SCR BlueBox having U-shape and V-shape shows perfect control of the flow turbulences. They finds that appropriate liquid Adblue/DEF injection was essential to achieve high level of NH_3 distribution and low back pressure.

Park T., *et. al.*, (2014), [38], investigated numerically using 3D numerical simulations, the pressure drop and flow mixing characteristics for SCR applications in order to develop an efficient static mixer. From their work, it was found that swirl type mixer is more appropriate than line type mixer. Static swirl type mixer in SCR system provides better flow mixing, approx. 18% better uniformity, swirling & turbulent flows.

Peters A., *et. al.*, (2015), [39], develops the relation between the static mixers in the exhaust system of a vehicle. The static mixers are having plurality of flow guide elements that influences the flow of exhaust gas stream and these static mixers are inclined at a given angle w.r.t. the mixer plane and are held in the exhaust gas channel with at least one retaining strip. They found that a minimum of one retaining strip is made resilient in partial regions and/or is elastically supported in the plane of the mixer.

Reitz R., *et. al.*, (1999), [40], incorporated a discharge coefficient model in order to predict initial behaviour of injected spray, for given ambient environments inside spray bomb and the nozzle geometry. Additional Rayleigh-Taylor hybrid model enhance the temperature dependency of liquid penetration. Rosin-Rammler distribution tries to increase drop size range in spray, thus at lower ambient densities, it increases the liquid penetration. The use of KH-RT model simulations to predict both hollow-cone spray behaviour and diesel jet behaviour will simplify atomization sub-models and improve multi-dimensional modelling.

Sala R., *et. al.*, (2017), [41], identifies the influence of dosing of vaporized UWS in SCR. They evaluated the effect of UWS preparation of NOx conversion in SCR catalyst. They investigated that the urea injection is critical at the low exhaust gas temperature. The preparation of UWS accelerates the urea thermal decomposition and thus increases NOx conversion efficiency by making reduction in urea consumption. From this, they designed a customized gas-urea system which considerably increased the NOx conversion in the SCR catalyst as compared with liquid urea dosing.

Salanta G., *et. al.*, (2010), [42], performed systematic design enhancements for enhancing emission reduction efficiency, by developing new injector mounting positions and multiple urea mixers, they were tested both by CFD Analysis and full scale lab tests. They perform CFD modelling, emission testing and mitigation strategy for comparing performances and

development of efficient Urea-SCR. The system is found to have a dominant influence on injector, its mounting configurations, mixer position & length, and end cone design.

Seo J., (2011), [43], investigated the different factors that influences of urea deposit using CFD. By using of TRIZ method (Taguchi Method) that performs the correlation analysis between design components for preventing the wall wetting and NOx reduction rate. They found that the urea deposit inside the convertor reduced from 135g to 11g on crystallization.

Sharma S., *et. al.*, (2017), [44], investigated that due to the low freezing point of DEF at -11°C, it becomes difficult for having NOx under the regulatory limit after 70 min of starting of engine. They compared the selected models that predicts the melt volume with time in case of vertical heating for different aspect ratios, shapes (having cylindrical or rectangular enclosures) and tank sizes. They identified a hybrid approach that predicts the melt volumes. They found that at Rayleigh Number (Ra) $2.5X10^{10}$, maximum error of 10% is predicted, after which the gap between experimental & predicted values increases significantly. For Rayleigh number range 10^{10} to 10^{13}, there is an error in prediction which limits to maximum error of ~17%. For the horizontal cylinder (or circular pipe), the melt volume prediction comes out with a maximum error of 15%.

Sheong H.J., (2012), [45], simulated a catalytic fixed bed reactor in 2D COMSOL for reaction. The model describes NO removal trend w.r.t. temperature and is compared with the Chae et al. kinetic model. The model shows with variations in NO and NH_3 ratios, below 350°C there is no increase in conversion of NO. There is slight increment above 400°C, hence ratio should be controlled taking into account NO conversion and NH_3 slip at specific temperatures. Also, there is no effect of porosity in the reactor for the NO conversion.

Way P., *et. al.*, (2009), [46], tries to optimize urea doser by using best practices for packaging in order to enable lot of system changes & improvements and maintaining or enhancing performance of NOx reduction. Thermal removal of deposits of urea, cyanuric acid, and biuret is a very slow process with maximum rate 2.0 mg/min at 600°C. By redesigning of doser and inclusion of UWS redirection device is required for eliminating deposits on downstream pipe walls. They found increase in NOx reduction from 47% to 80%.

Wiesche S., (2007), [47], efficiently use CFD and numerical heat transfer methods in the development and optimization of automotive SCR-tank systems. They uses thermal simulations that include the phase changing of UWS (melting and freezing), heat conduction, power generation, and natural convection effects within the liquid. They validate this numerical

scheme by comparing them with benchmark cases and experimental data. They finds that due to the mushy region, the total freezing time of urea within a tank is mainly governed by heat conduction.

Wu B., *et. al.*, (2014), [48], simulates the species concentration and flow distribution inside the decomposition chamber and find out that recirculation of excessive ammonia is the major reason behind the debris formation at the chambers top. They recommend introduction of flow baffles to differentiate urea flow from upper chamber in order to resolve the issue.

Wu Y., *et. al.*, (2017), [49], studies the effects of structural parameters such as catalyst length, catalyst c/s area, substrate wall thickness, CPSI thickness, coating thickness and their effects on SCR performance in order to optimize the system. They calibrated the kinetic parameters of the SCR reactions. They also optimized the structural parameters in exhaust gases flow using the Response Surface Methodology (RSM) and finds out the pressure drop. Using CFD they verified the optimal structural parameters and finds out the catalyst volume remained after the reaction, NOx conversion rate and effectiveness of the optimized process.

Zheng G., *et. al.*, (2014), [50], had investigated in the direction to achieve both low cost and compact space UWS-SCR system, and proposed an unconventional design in which injector is closely coupled with SCR can. To resolve the issue of low conversion & ammonia slip due to short distance between SCR substrate and injector and the issue of formation of urea deposit. They proposed solutions as 1) use of dual perforated baffles which provides unique flow pattern. 2) use of single perforated baffles and two stage mixer. They perform CFD simulations and modelling for finding the optimum design in which dual perforated baffle proved to be the better one.

3.3 Gaps Identifications:

Literature shows many aspects but we got a very little information about the internal process occurred in the Urea SCR System. We need to proceed in the direction to find the flow uniformity when the urea gets mixed with the exhaust gases. The effect of surroundings on heat and mass transfer leading to the temperature change is also required to find out. Also, when the urea injection process is going on, how different parameters such as length of Catalytic convertor, Convertor insulation, exhaust mass flow rate , Turbulency and swirling are affecting the spray droplet. The effect of spray at different temperatures are also not very clear from the research papers thus proper simulations in these direction are to be find out. These simulations

will help us in understanding the Evaporation tendency of UWS and how the wall film is formed due to this evaporation can be investigated.

3.4 Challenges of controlling automotive Urea-SCR systems

The design objectives for Urea-SCR system, according to BS-VI emission standard are focused upon minimizing the NOx emissions and minimizing the NH_3 slip.

Due to the transient behaviour of engine combustion in automotive applications, the use and control of Urea-SCR system involves many challenges. Low operating temperature, flow variations, poisonous species present in catalyst, temperature fluctuations and mechanical vibrations are certain factors that are influencing the system [51].

Also, the degeneration of catalyst over time degrades their efficiency. In order to overcome these challenges, a controlling action needs to be defined. Throughout a driving cycle, the variations in the engine load results in the continuous change of exhaust flow composition, flow rate and temperature. From the diesel engine combustion characteristics, we can say that during the low load periods, the temperature of exhaust gas is low. The reactions in the SCR catalyst are directly influenced by this low exhaust temperature as these catalyst are slower for typical composition of exhaust gas at low temperatures.

At low temperatures, there is lower NOx conversion and at high temperatures, there is a high risk of ammonia slip. Thus, we can say that temperature variation has a substantial influence on the performance of the system. After seeing that NH_3 storage potential temperature is dependent on temperature, it is essential to keep the NH_3 below the steady state storage capacity at low catalyst temperatures. This will prevent the high ammonia slip at large temperature gradients. All these parameters complicates the controlling process of Urea-SCR. Hence, for having a balance between the ammonia slip and NOx reduction, the advanced control of reductant injection is important.

CHAPTER 4

MATHEMATICAL MODELLING IN UREA - SELECTIVE CATALYTIC REDUCTION SYSTEM

All simulations have some background upon which the whole system is working. There is a need to understand this basic mathematics that runs in the background of simulations during our research work. In order to find the influence of urea droplet and the exhaust gases on the heat and mass transfer of the system we need to deal with the dynamics of the droplet, temperature dependency on the system, effect of evaporation of the droplet and the heat losses inside the sub-system. All these parameters were elaborated as follows in this section.

4.1 Droplet dynamics

From [53], we can find the droplet dynamics occurring in the urea bubbles is described in this section. As Droplet motion influences the heat and mass transfer occurring between exhaust gas and the droplet, thus we need to take concern of this droplet motion. Initially the flow is considered to be in one dimension, and the initial velocity of the droplet is treated parallel to the flow direction. The differential equation for the droplet velocity and the trajectory of the droplet is

$$c_{p,Substrate} = S_1 + S_2 T_{SCR} + S_3 T_{SCR}^2 \tag{4.1}$$

Drag force is the controlling force in the UWS injection. Due to one dimensional assumption, the buoyancy forced are not considered. Hence, the droplet motion is expressed as:

$$m_d \frac{dv_d}{dt} = \sum F = F_d \tag{4.2}$$

Drag force can also be expressed as:

$$F_d = C_d \{\frac{\pi D_d^2}{4}\} \{\frac{\rho_d \mid v_g - v_d \mid (v_g - v_d)}{2}\} \tag{4.3}$$

where C_d is the drag coefficient, a function of the droplet Reynolds number Re_d.

Droplet Reynolds number Re_d can be expressed as:

$$\mathrm{Re}_d = \frac{\rho_{mix} \mid v_g - v_d \mid D_d}{\mu_{g,mix}} \tag{4.4}$$

Hence, the combined momentum equation of the droplet is expressed as:

$$\frac{dv_d}{dt} = \frac{3\rho_g c_d}{4\rho_d D_d} | v_g - v_d | (v_g - v_d) \tag{4.5}$$

As the mass of the droplet is negligible in comparison with the mass of exhaust gases in the SCR system, thus we neglected the momentum transfer from the droplet to the exhaust gases. So, there is no effect of the droplet motion on the exhaust gases.

4.2 Temperature Model

From [28], we can find the temperature modelling to find the specific heat constant for the system and temperature variations. In temperature model we assume that the SCR is properly insulated and there are minimum heat losses in the surroundings. Thus, we neglect the radiative and convective losses to the surroundings. Hence, the temperature model by the following equation:

$$T_{SCR} = N_{cell,T}\{\frac{m_{exh.gas} c_{p,exh.gas} (T_{exh.gas} - T_{SCR})}{m_{SCR} c_{p,SCR}}\} \tag{4.6}$$

The SCR monolith and the exhaust gas specific heat capacities are taken to be the function of temperature. As a function of temperature, the modified specific heat constant for exhaust gas is expressed as:

$$c_{p,exh.gas} = EG_1 - \frac{EG_2}{T_{exh.gas}^2} + EG_3 T_{exh.gas} + EG_4 T_{exh.gas}^2 \tag{4.7}$$

where EG_1, EG_2, EG_3 and EG_4 are constants specific to exhaust gas.

In the beginning, this temperature model was comprised of 3 cells. When this temperature model was compared with the test data, it was found that this temperature model gives good results with the real system, but in order to achieve far better results, we require some modifications. So, by lengthening the number of cells to 9 and discretizing them to 3 cells of temperature model, in order to the capturing of reaction kinetics, the temperature profile through this temperature model captured the better results related to dynamics of real SCR system as shown in figure 4.1.

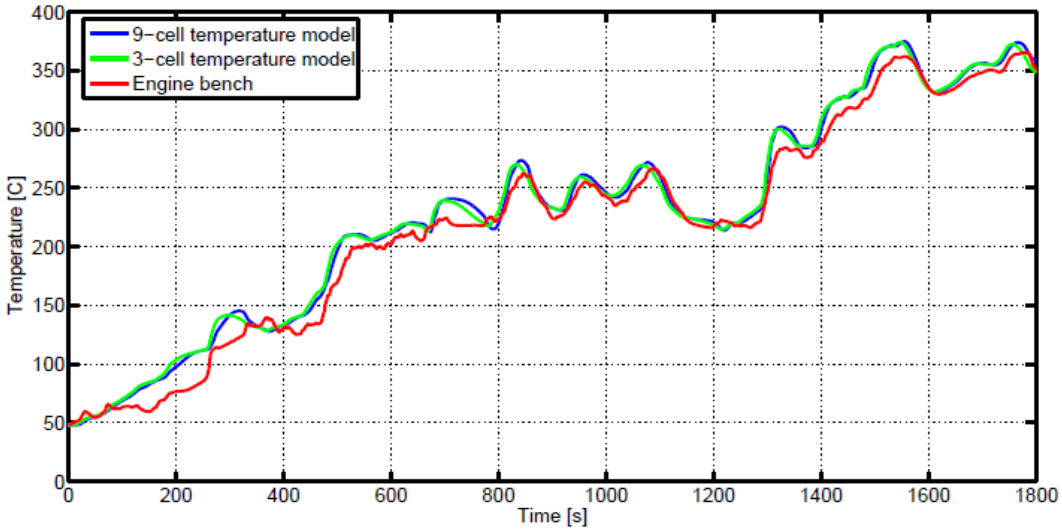

Figure 4. 1 3-cell vs 9-cell temperature model

Similarly, as a function of temperature, the modified specific heat constant of the substrate

$$c_{p,substrate} = S_1 + S_2 T_{SCR} + S_3 T_{SCR}^2 \tag{4.8}$$

where S_1, S_2 and S_3 are constants specific to the substrate material.

4.3 Evaporation model

This evaporation model is based on Abramzon - Sirignano model, [26] and following few assumptions were made for simplifications.

1. The geometry of the droplet is spherical and is symmetric:
2. The surface of the droplet is surrounded by a quasi-state, steady gas film.
3. Both phases of liquid and gas that are surrounding droplet are in thermodynamic equilibrium.
4. The rapid mixing (RM) model is used in order to provide uniform concentration, temperature, and fluid properties in droplet [53].

From the UWS, water evaporates first, due to its lower boiling temperature. From Abramzon-Sirignano model, mass transfer equation is:

$$\frac{dm_d}{dt} = -\pi D_d \rho_{g,mix} \tau_{ref} Sh_c \ln(1 + B_M) \tag{4.9}$$

Considering that depending upon the ambient temperatures, UWS droplet behaves differently at different temperatures, we adjust the exhaust temperature with an adjusting temperature coefficient (T_∞/673). So, the mass transfer equation can be expressed as:

$$\frac{dm_d}{dt} = [-\pi D_d \rho_{g,mix} \tau_{ref} Sh_c \ln(1+B_M)]\{\frac{T_\infty}{673}\} \tag{4.10}$$

Thus, the heat transfer rate is expressed as:

$$\frac{dT_d}{dt} = \{\frac{\frac{-dm_d}{dt} c_{p,ref}(T_g - T_d)}{B} - L\} \frac{1}{m_d c_{p,AdBlue}} \tag{4.11}$$

B_M is the Spalding mass transfer number, while B_T is the Spalding heat transfer number.

$$B_M = \frac{Y_{vap,S} - Y_{vap,Y}}{1 - Y_{vap,S}} \tag{4.12}$$

$$B_T = (1+B_M)^{\phi} - 1 \tag{4.13}$$

$$\phi = \frac{c_{p,vap} Sh_c \, \mathrm{Pr}_{ref}}{c_{p,mix} Nu_c Sc_{ref}} \tag{4.14}$$

Sh_c is modified Sherwood number while Nu_c is the modified Nusselt number.

4.4 Urea decomposition and Heat losses from the exhaust pipe

From [29], as the temperature sensor gets wetted with the urea droplets, it results in the error in temperature measurements. Hence, to have a fair estimation of inlet temperature of SCR, we need to model and compute the heat losses through the urea pipe and resulting from urea decomposition.

When the urea is injected into the SCR upstream, due to the high temperature of exhaust gases, it gets reduced into iso-cyanic acid and ammonia. The evaporation of water causes lowering the exhaust gas temperature. The heat losses from the urea decomposition expressed as:

$$Q_{AdB} = m_{Urea}[c_{p,H_2O(l)}(T_{b,H_2O} - T_{amb}) + L_{v,H_2O} + (1-\gamma)c_{p,H_2O}(T_{out} - T_{b,H_2O}) + \gamma C_{p,Urea}(T_{out} - T_{amb}) \tag{4.15}$$

The heat losses from the exhaust gas are expressed as:

$$Q_{exh.gas} = c_{p,exh.gas}[m_{exh.gas} T_{in} - (m_{exh.gas,US} + m_{Urea}) T_{out}] \tag{4.16}$$

Heat losses due to urea decomposition, occurs through the exhaust pipe. These heat losses in pipe are further divided into internal & external heat losses. The external heat losses involves the heat losses to the surroundings due to convection and radiation phenomenon, while the internal heat losses occurs due to exhaust gas to the pipe walls. These internal and external heat losses occurs at the outlet of the exhaust pipe and are expressed as:

$$Q_{external} = A[h_{CV,ext}(T_{wall} - T_{amb}) + \sigma_{SB}\varepsilon_{rad}F_v(T_{wall}^4 - T_{amb}^4) \quad (4.17)$$

$$Q_{external} = h_i A(T_{exh.gas} - T_{wall}) \quad (4.18)$$

The wall temperature of the exhaust pipe can be expressed as:

$$\frac{dT_{wall}}{dt} = Q_{internal} - Q_{external} \quad (4.19)$$

The radiation factor can be expressed as:

$$Q_{radiation} = A[\sigma_{SB}F_v\varepsilon_{rad}(T_{wall}^2 + T_{amb}^2)(T_{wall} + T_{amb})(T_{wall} - T_{amb}) \quad (4.20)$$

$$Q_{radiation} = h_{radiation}(T_{wall} - T_{amb}) \quad (4.21)$$

where $h_{radiation}$ term is a lumped non-linear term and can be used for comparing the coefficients of heat transfer respectively.

The partial differential equations are used for finding the temperature drop in the exhaust pipe. Let us consider a small section of pipe of length dx in the straight pipe of length L, at a distance (x + (dx/2)) from the inlet of the pipe.

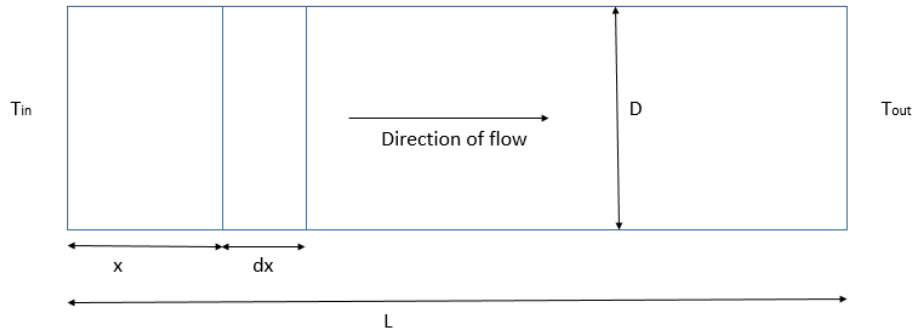

Figure 4. 2 Pipe considered for derivation

Since the temperature of the exhaust gases decreases along the length of the pipe as these exhaust gas flow passes through the pipe. Let the temperature be T_s at the end of the small section. The surface area of the small section is:

$$\frac{dm_d}{dt} = -\pi D_d \rho_{g,mix} \tau_{ref} Sh_c \ln(1 + B_M) \quad (4.22)$$

Thus the heat flux through this small section is:

$$Q = A_s h_s (T_s - T_{wall}) \quad (4.23)$$

Heat lost from the exhaust gases at the beginning at a distance ($x-\frac{dx}{2}$) and at the end of the section ($x+\frac{dx}{2}$)

$$Q = m_{exh.gas} c_{p,exh.gas} (T_{x+\frac{dx}{2}} - T_{x-\frac{dx}{2}}) \tag{4.24}$$

Considering the limit as dx ► 0, the PDE obtained is:

$$\frac{dT_{wall}}{dx} = \frac{h_s \pi D (T_s - T_{wall})}{m_{exh.gas} c_{p,exh.gas}} \tag{4.25}$$

Using method of separation of variables and solving for the outlet temperature of the pipe the following final expression is obtained:

$$T_{pipe-out} = T_{wall} + (T_{exh.gas} - T_{wall}) e^{(\frac{-h_{cv,i} A_{pipe}}{m_{exh.gas} c_{p,exh.gas}})} \tag{4.26}$$

The pipe model along with the model for urea decomposition is coupled with the SCR model and is used to obtain an estimate of the SCR temperature.

CHAPTER 5

MODELLING AND ANALYSIS USING COMPUTATIONAL FLUID DYNAMICS

In automobile exhaust systems, because of high thermal stresses, common failures occurs at aggregate level or at component level. There is very high temperature gradient near both the inner and outer inlet cone and at the junctions between the pipes. A precise temperature distribution is required for simulating the distribution of thermal stresses near the critical areas mentioned.

Since the experimental process of evaluation of SCR exhaust performance that includes the measurement of NH_3 concentration at inlet of SCR-Catalyst, which is a difficult, expensive and time consuming task. Several Numerical techniques and Computational methods had been developed that enables simulations done on CFD Fluent to predict the chemical reactions and atomization occurs in SCR system, simultaneously with flow mixing. CFD Fluent simulations will save a lot of time in the development of prediction of flow uniformity [24].

CFD is an important tool for designing & developing aggregates in automobile industry. Due to above mentioned concerns, Exhaust after-treatment systems are designed and developed based on CFD results, irrespective of application, the released NOx must lie within the permissible limits.

CFD Ansys is the best tool available for the analysis of temperature distribution at critical areas and high temperature gradient. Along with the conjugated heat transfer, CFD can correctly calculate the temperature distribution of CATCON, including the muffler and convertor assembly. The muffler assembly consists of perforated baffles and pipes, while convertor assembly consists of insulations of cone, airgap, etc.

3-D CFD method is proved to be a reliable, time and money saving tool to evaluate and optimize flow distribution for catalytic converter.

Back-pressure, substrate durability and conversion efficiency of emission targets are highly dependent on the distribution of exhaust flow inside the substrate. Simultaneously, for preventing any damage as a result of high temperature, a special care must be taken for thermal management in SCR exhaust system.

For best results, approach and parameters used in C.F.D. modelling for Urea-SCR as shown in figure 5.1:

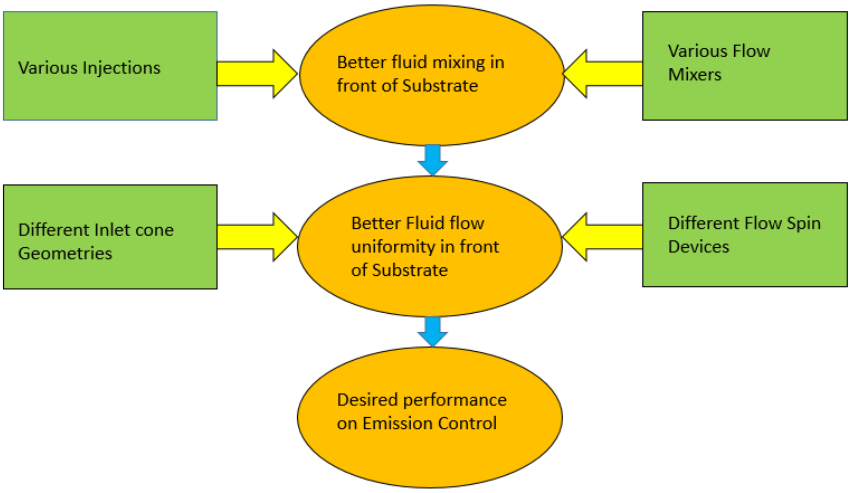

Figure 5. 1 Factors affecting the efficiency of NOx Conversion in SCR.

Usually, a Catcon have inlet and outlet cones, ceramic substrates, one convertor shell and one insulation mat. The total pressure loss in the system is the sum of pressure losses comes through the inlet & outlet cones, flow passing from substrate and flow re-distribution devices for e.g. perforated baffles and flow mixers. Thus, for optimizing the total pressure inside the system 3-D CFD is a very effective tool. The pressure losses from the inlet & outlet cones are optimized by optimizing their geometries which reduces bulk recirculation and improves flow uniformity along with reducing the turbulence in the flow.

5.1 3-D Mesh Generation, Boundary Conditions & Numerical Methods

CFD numerically simulate the species transportation, fluid flow (both turbulent and laminar), two-phase flow, and combustion and conjugated heat transfer (all conduction, convection and radiation).

As the mainstream in mass fraction of exhaust gas are nitrogen, considering the exhaust gas to be an ideal gas. For an ideal gas the density changes with static pressure and local gas temperature. For the exhaust gases, heat capacity and thermal conductivity along with the capacity and conductivity of the insulation material are taken to be the function of temperature.

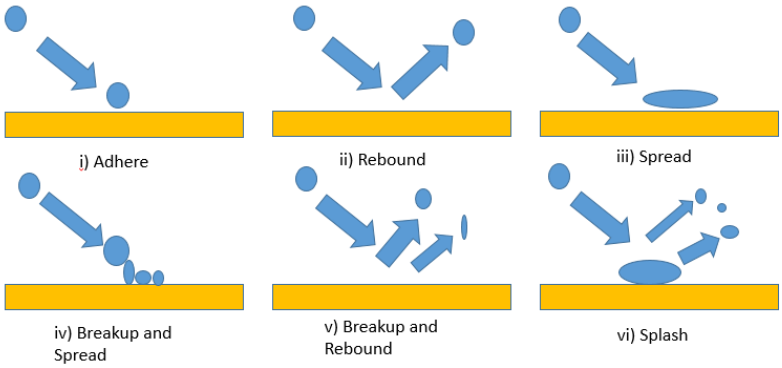

Figure 5. 2 Possible outcomes of droplet impingement on Solid wall

There are various possible outcomes of droplet impingement on solid wall which is shown in figure 5.2. CFD Fluent computes the thermal conductivity & heat capacity of the material, heat transfer between the wall and the fluid flow, heat convection and radiation. As the flow inside the pipe is basically a turbulent flow, so we used k-ε turbulent model in Ansys Fluent. Bulk flow is treated as laminar flow. Through the substrate, depending upon cell structure the pressure drop can be expressed as:

$$\Delta P_{lateral} = me^{10}(\mu v) + ne^{3}(0.5\rho v^{2}) \tag{5.1}$$

$$\Delta P_{axial} = me^{7}(\mu v) + ne^{3}(0.5\rho v^{2}) \tag{5.2}$$

CFD meshing is the factor that can alter the results. Depending upon the operating conditions, such as rate of urea injection and exhaust gas velocity, mesh size is defined. Time step is important for transient CFD calculations. A small time step automatically increases the computational time but provides stabilize and converged results. A large time step decreases the computational time but provides divergence in results. Thus, to achieve both non-diverged results and declination of computational time, usually a time step of around 2 to 5 degree is used.

For confirming accuracy in the CFD results, we need to have a high quality mesh. Since mesh plays a vital role in CFD analysis, thus an independent study is required for achieving good results. Generally, the CFD results for e.g. temperature, pressure and velocity curves plotted, are dependent on mesh sizes. When the absolute value of the slope is smaller than 0.50, a satisfactory mesh size is attained. With the decrease in mesh size, the graph reaches to its asymptotical value. With each mesh refinement, there is a 0.50% accuracy in the CFD Results. For certain critical components for e.g. Catcons & flow mixers, we requires very fine meshes. While at some places for e.g. pipes & substrate, we requires hexahedral meshes to save

computational time. Due to geometrical complexity, tetrahedral meshes are used for the inlet cone and the outlet cone.

Usually, the whole after-treatment system results in more than 0.5 million cells if we use the 2mm to 5mm mesh size. For reducing the computational time lapse for large number of cells for larger domains, we use the coarse meshes in the center of the domain. For predicting the forced convection coefficient and pressure loss across the converter system and across the solid-air interface, we built 0.5mm to 2mm prisms common with three layers.

Generally, the inlet boundary conditions in the exhaust system are exhaust temperature, length scale, mass flow rate of gases, turbulent intensity at inlet. For pressure loss calculations, boundary conditions for pressure at exhaust outlet is specified. Ambient temperature along with the material's emissivity is used for predicting the skin temperature.

5.2 Important Numbers used in Simulations

5.2.1 Uniformity Index of the flow is used to find the degree of flow distribution in the front of the substrate. It is expressed as:

$$\gamma = 1 - \int_{A_0} \frac{\phi}{(2U_{avg}A_0)} dA \tag{5.3}$$

where $\phi = ||U| - U_{avg}|$ and $U_{avg} = \int_{A_0} \frac{U}{A_0} dA$

The maximum value of U.I. can be 1.

5.2.2 Local velocity deviation index demonstrates the deviation from average velocity and is expressed as:

$$D_{ev} = \frac{||U| - U_{avg}|}{U_{avg}} \tag{5.4}$$

5.2.3 Velocity deviation index demonstrates the overall behaviour of flow uniformity inside the substrate as following:

$$D = \frac{\int_{A_0} \frac{||U| - U_{avg}|}{U_{avg}} dA}{A_0} \tag{5.5}$$

5.2.4 Flow mixing index: Similar to the flow uniformity index, we define a parameter which is used in finding the degree of mass distribution across the section plane which is perpendicular to the direction of bulk flow, this index is known as the flow mixing index, which is expressed as:

$$\tau = 1 - \int_{A_0} \frac{|C - C_0|}{2A_0C_0} dA \tag{5.6}$$

where C_0 is the ammonia mass concentration through the plane A_0.

$$C_0 = \int_{A_0} \frac{C}{A_0} dA$$

5.3 Parameters Considered for Input

There are several parameters which are controlled, manipulated and disturbed in the urea-SCR system. The controlled variables are NH_3, NO and NO_2 concentration at the outlet. The urea (ammonia) injection rate can be manipulated. While the concentration of NO, NO_2 along with the temperature and mass flow rate of exhaust gas are the variables creating disturbance in the process.

5.3.1 Input Parameters

1. Injecting Liquid: Urea-Water Solution
2. Duration of Injection, t = 8-12ms
3. Height of injection, h = 30mm
4. Pressure for injecting UWS, P_{inj} = 4.7bar
5. Temperature for injecting UWS, T_{inj} = 298K
6. Temperature at Wall, T_w = 333K, 393K, 453K, 513K, 573K.
7. Hole dia. of injecting nozzle, d_{inj} = 0.5mm
8. Angle of injection, $\theta = 90^\circ$
9. Half Cone Angle, $\phi = 28^\circ$
10. Ambient Temperature and Pressure, T_{amb} = 298K and P_{amb} = 1bar.

5.3.2 Simulation Conditions for the injectors and sprays

The Eulerian-Eulerian and Eulerian-Lagrangian models are used for multi-phase flow modelling due to their better exactness in output values. Eulerian-Lagrangian model is used over the Eulerian-Eulerian model because it provides a thorough information about discrete behaviour of particle and not through continuum dynamics. Also, Eulerian-Lagrangian model becomes more computationally cheaper during multi-equations are used.

The Eulerian-Lagrangian modelling defines problem in two different concepts: a) particle treated as individual droplets, b) particles treated as bundle. In the Eulerian-Lagrangian approach, the interaction between the particles are modelled with continuous phase and using unsteady and incompressible flow Reynolds Averaged Navier Strokes (RANS) equations. Realizable k-ε model is used for estimating turbulent flow values. In calculating the velocity and thickness of fluid film formed due to primary spray atomizer, Linearized instability sheet atomization (LISA) model is used.

For having accurate results in Urea-Water spray analysis, an excellent mesh is generated using automatic meshing techniques in ANSA 17.0 with volume mesh of 5mm base size. We used the prism layers, as they resists the numerical diffusion, thus gives more accurate results for finding heat transfer and flow separation near the walls.

5.4 Urea injection for SCR system

In the exhaust system, it is a very time and money consuming process in experimentally finding the NH_3 concentration in front of SCR substrate.

CFD simulations are a very helpful tool in complicated calculations where two-phase flow and species transportation are involved. Certain areas of our interest that involves CFD are urea injection angle and location, droplet size, its evaporation and its distribution, injection velocity and flow mixing.

5.5 Effect of Transient and steady state CFD simulations

Transient CFD simulations are used for designing and optimizing exhaust subsystems such as exhaust manifold and pipe junctions. Variable mass flow rate and variable temperature effect is investigated for finding total pressure loss.

From transient CFD simulations analysis, we observed that the Flow uniformity index

a) Varies with the crank angle of the engine.
b) Increases with increasing local mass flow rate.
c) Reaches up to 98% during highest flow rate, whereas reaches up to 64% during lowest flow rates.

During steady-state CFD Simulations, we find that the uniformity index is inversely dependent on the mass flow rate, means it decreases with increasing mass flow rate.

This ambiguity between the two simulations is due to the runners and substrate. During steady state, mass flow is only defined for one runner without the air flow in other runners, while in transient state, the downstream flow from one runner have definite effects on the static pressure of the other runner at the bank.

CHAPTER 6

RESULTS, DISCUSSION & CONCLUSIONS

Generally, an integrated exhaust system consists of DOC, DPF and SCR. This system have various flow paths in parallel substrates and return lines. 3-D CFD Analysis is used in such complex systems for finding the flow distribution inside the substrate. This flow distribution is dependent upon inlet locations, location of substrates and chamber geometry. The Flow streamlines gives brief understanding about the flow separation and its rotation.

CFD Simulations also gives brief information about the division of mass flow of exhaust in multi-path systems. Ideally, from each sub path, same mass flow rate is preferred.

Velocity deviations and magnitudes inside integrated DOC, DPF and SCRis shown in figure 6.1, while Flow streamlines showing separation and flow rotation in SCR system with two substrates in parallel are shown in figure 6.2.

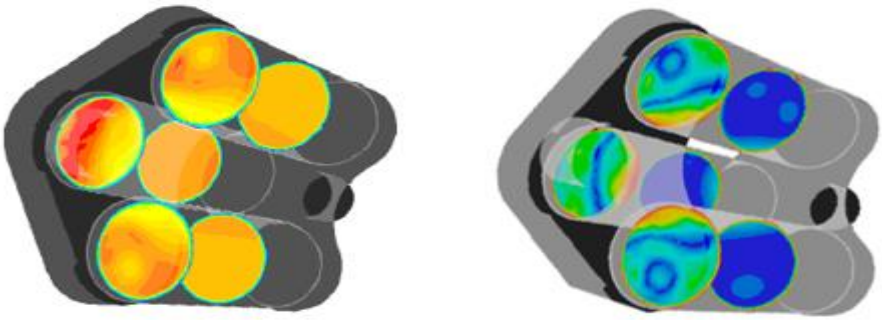

Figure 6. 1 Velocity deviations and magnitudes inside integrated DOC, DPF and SCR

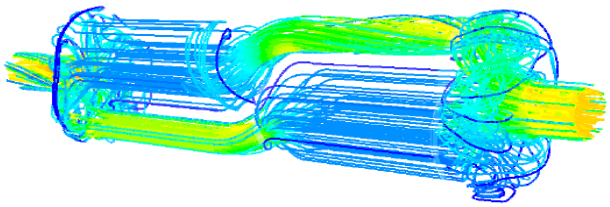

Figure 6. 2 Flow streamlines showing separation and flow rotation in SCR system with two substrates in parallel.

6.1 Estimation of Flow uniformity

Some cases in exhaust system, requires very high flow uniformity. To reduce the heat losses through the exhaust pipe, all substrates are combined to form one integrated system. Thus, for increasing the flow distribution, one flow redistributor is implemented.

Depending upon the geometry, the value of uniformity index varies. Inlet cone affects the uniformity index more than the outlet cone. Inlet cone with cone angle 0˚ have best flow uniformity index of 0.935 and this will reduce to 0.912 at cone angle of 60˚. The maximum flow uniformity index is achieved with a combination of outlet and inlet cone angles and their orientations.

6.2 Effect of Insulation of Convertor Cone

Insulation of the convertor cone does not affect the central cell skin temperature. While the insulation on different cones especially at the inlet cone affects the skin temperature as shown in figure 6.3. The skin temperature near the inlet cone is found to be around 680℃ to 720℃.

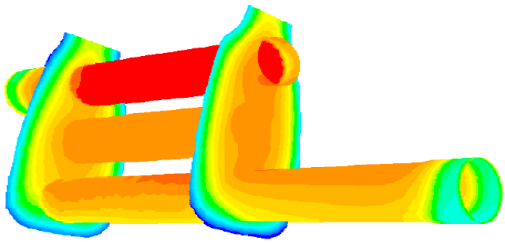

Figure 6. 3 Distribution of Skin temperature inside the muffler

6.3 Effect of mass flow rate of Exhaust and inlet cone length

The mass flow rate of exhaust and length of inlet cone are simulated for knowing their effects on flow uniformity index and pressure loss. Very minimal change in flow uniformity index is seen through rotating the angle cones along the smaller axis. But a good improvement in flow uniformity index is seen by shifting the plane of the flow inlet by 10mm, 20mm and 30mm from geometrical centre along the larger axis. The maximum flow uniformity index is found when the flow inlet plane is at rotation angle of 20˚ and is 30mm shifted geometry.

Both the static pressure and exhaust gas temperature varies depending upon the flow path. Temperature decreases rapidly from turbocharger (nearly 750℃ to 1100℃) to exhaust tail-pipe (nearly 150℃ to 350℃). The higher gas density due to lower temperature results in reduced pressure loss through the component. Thus, a conjugated heat transfer model is choosed to enhance accuracy.

6.4 Effect of Flows: An overview to Turbulent and Swirling flow

To understand the flow mixing phenomenon, 3-D numerical simulations were executed with a flow mixer of delta wing shape placed just before the SCR system.

A bulk swirling flow is generated by using delta wing blades twisted at certain angle as shown in Fig. 6.4 (a).

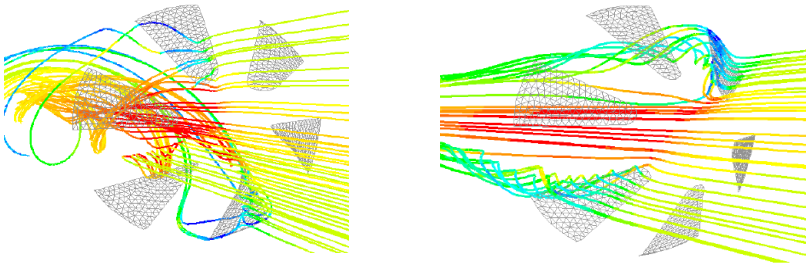

a) b)

Figure 6. 4 Effect of flow mixers

Intentionally, a turbulence is generated through the flow mixer having six delta wing blades as shown in Fig. 6.4 (b).

From the simulation results we had found that by using the delta wing shaped mixer, an improvised mixing pattern is achieved. Straight blades mixer displays higher flow mixing index in downstream. For a shorter distance, a small turbulance is created by the straight blades that enhances mixing. For longer distance, the bulk swirling helps in mixing improvisation. Hence, we need to optimize the flow mixer for attaining the minimum pressure loss in the exhaust gases. Depending upon the film thickness, the wall film is colour coded.

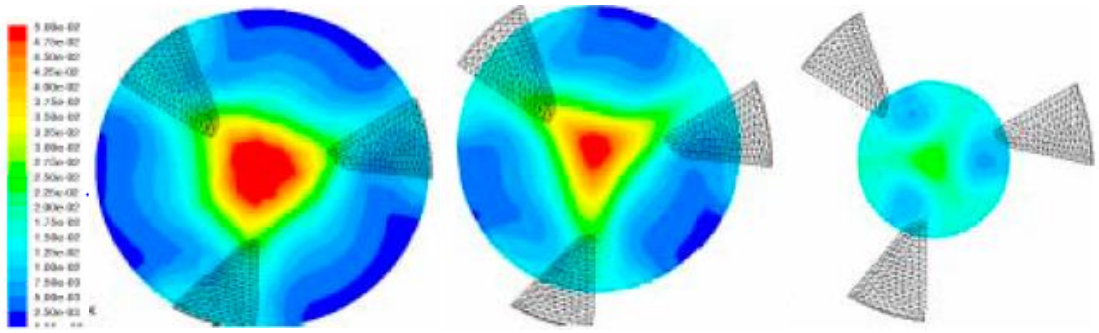

Figure 6. 5 Mass concentration of ammonia between flow mixers along with 3 twisted blades at a distance from flow mixer a) 80mm, b)150mm, c) 220mm

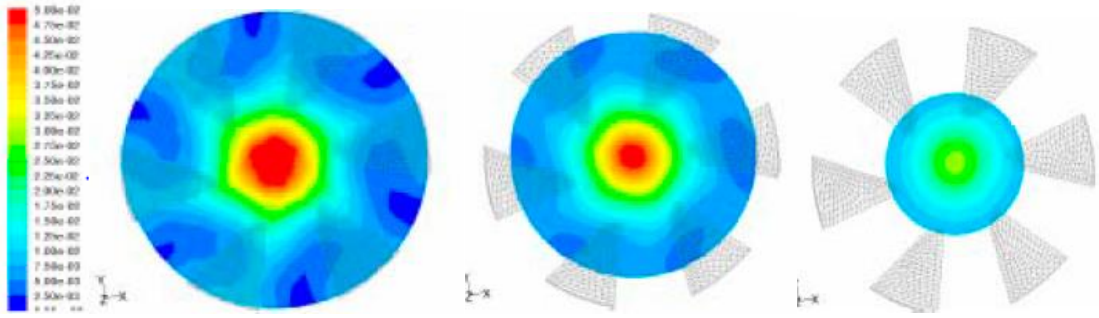

Figure 6. 6 Mass concentration of ammonia between flow mixers along with 6 twisted blades at a distance from flow mixer a) 80mm, b)150mm, c) 220mm

In order to improvise the flow mixer's performance, from the above diagrams we find that the as the injector get moves away from the mixer,the cross-section tends to become smaller, hence we conclude that 3 twisted blades flow mixer shows massive reduction of additional pressure loss from 125 mbar to 51 mbar as compared with 6 twisted blades flow mixer. Also, 3 twisted blades flow mixer shows higher flow mixing index by 7%-8% as compared with 6 twisted blades flow mixer are shown in figure 6.5 and figure 6.6 respectively.

6.5 Effect of different geometries in injection system

When a flow mixer is added in the flow stream, back pressure of the system increases. So, to avoid this, a concept injector that can optimize the urea injector itself is developed as shown by figure 6.7. The concept injector has a ring like shape, which reduces the injection pressure and improvises the flow mixing. Simulations were performed for both ring type and tube injector in Ansys Fluent by considering the same inlet conditions and same boundary conditions. Results shows that the ring injector attains higher flow mixing index (around 18% to 20%) with a small pressure loss.

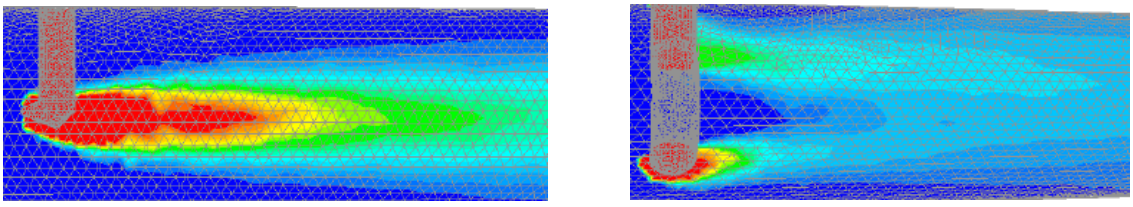

a) b)

Figure 6. 7 Ammonia distribution along the direction of flow using a) tube injector b) ring shaped injector.

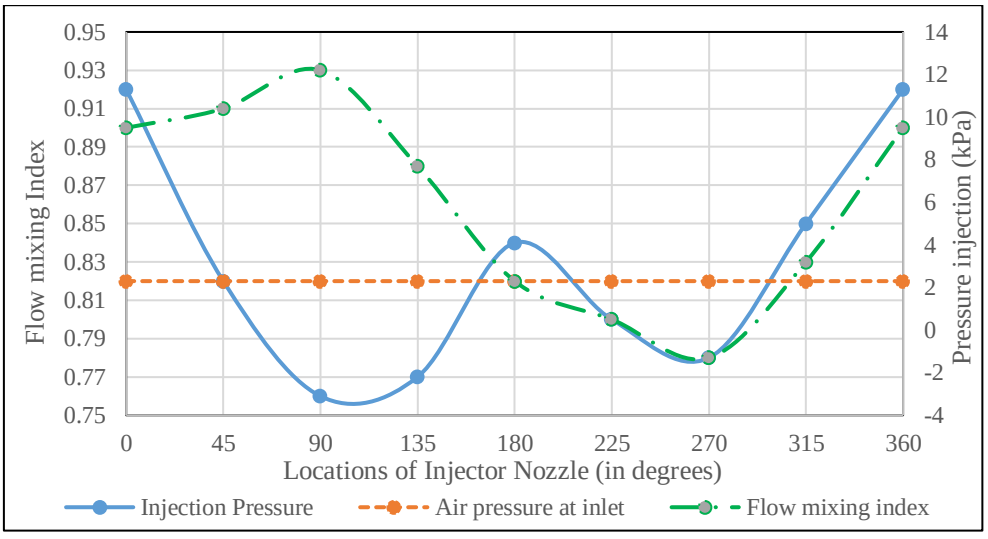

*Figure 6. 8 Different locations of Nozzle around the Injector**

*: Fictitious data to maintain confidentiality.

Separate simulations were performed to study the effect of the location of spray nozzle on injection pressure and flow mixing index as shown in figure 6.8. Both of these parameters varies with the location of nozzle. The minimum injection pressure as well as maximum flow mixing index are found when the nozzles are located at equal spacing on outer surface of the ring tube. The atmospheric pressure is found to be more than the minimum injection pressure. The front injection with significantly low mixing index and slightly higher injection pressure is used in order to evade the direct impingement of liquid UWS on exhaust pipe wall, because due to this, the exhaust pipe gets eroded.

For a tube injection system, the swirling flow gives better results in improvising the flow mixing index, while in case of ring injection system only a considered amount of improvement in flow mixing index is achieved. Injection pressure declines in tube injector system and increases in ring injector system with nozzles front located.

Usually the urea injection dosing unit is placed next to the bended pipe. But due to packaging constraint, the length of pipe is an issue. Some definite length of the pipe is required for attaining ideal mixing of ammonia in front of the substrate. So, an atomizer is placed next to the urea injector.

For estimating the performance of various flow mixing devices, we simulate them in CFD using the single phase flow with activated species transportation model. Properties of gaseous species for e.g. H_2O (vapor), O_2, CO, CO_2, N_2, NH_3 are defined. Boundary conditions at the inlet: first for exhaust gases at inlet and second for urea (ammonia) which is injected into the exhaust are defined. For fast and easy solutions related to mixing, turbulent flow and rotated bulk flow inside the different flow devices Simple method is used, but it does not gives better results in spray atomization, urea evaporation and decomposition. Multi species two phase injection system is used for conjugated heat transfer along with the chemical reaction model.

To achieve high NOx conversion, we requires better urea conversion which is possible from a uniform mixture of NOx & NH_3. For this, static mixers needs to be installed that enhances the break-up of urea spray into small droplets and to enhance turbulence.

Radial distance and axial distances of spray impingement were measured to find out the movement of the spray. From this wetting of wall can be easily found out. Due to the high exhaust gas temperature, the wall surface temperature increases and reduces the spray intensity. Hence, due to increased droplet evaporation, the wall wetting reduced.

6.6.1 UWS spray at low temperature (333K)

Impingements of droplet spray provides information about solid deposits and urea distribution. This can be predicted with the help of some parameters such as spray injection angle, droplet velocity and wall surface temperature.

After the injection, visual investigation of UWS spray at 333K is performed for different time intervals; at t = 1ms, 2ms,…, 10ms, as shown in figure 6.9. The spray front propagation, in both radial and axial direction, reveals the droplet atomization rate after impingement on hot contact surface of SCR and Exhaust gas. The solid deposit formation occurred due to the formation of fluid film, which is developed as a reason of more wall wetting due to impingement of large propagation of particles.

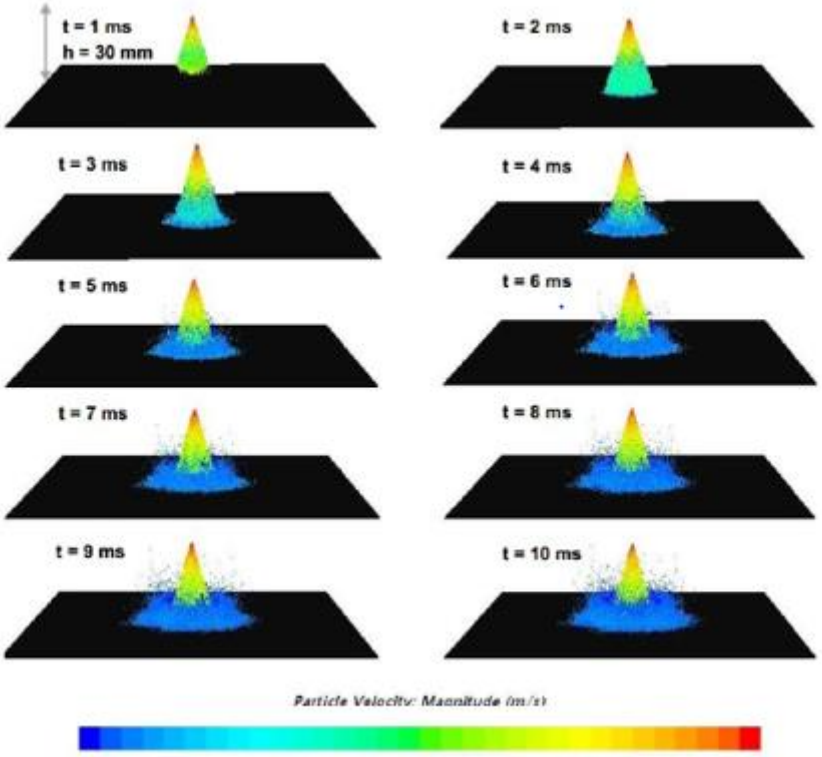

Figure 6. 9 Pattern of spray development at different times on heated wall

The wall temperature is lesser than the urea's melting point and thus UWS spray develops confined cooling at impingement area, making urea droplets adhered at the wall surface. This will led to urea crystallization after the water evaporation.

Both values of axial and radial distances after the impingement of ammonia are high enough and are analogous to experimental data performed earlier.

6.6.2 UWS spray at high temperature (573K)

Spray impingement at heated wall of wall temperature 573K was investigated for various times at t = 1ms, 2ms… 10ms. The height of urea injection is 30mm and is done at an angle of 90˚. When the UWS gets impinged on the surface, the momentum of urea droplet is transformed into three different components. These are

a) Momentum along the impingement surface by the front movement of the droplet.
b) Momentum loss occurred due to formation of secondary droplet after impingement.
c) Momentum loss occurred due to rebounding and thermal breakup.

The behaviour of spray wall interaction is dependent upon: wall temperature, Weber number of droplet, impinging droplet's rebounding and thermal breakup. Rebounding occurs in the normal direction to the exhaust pipe, providing more time to reductant for mixing and evaporation and making active substance production accelerated and hence, is a beneficial phenomenon for the occurrence of evaporation and reductant mixing with the exhaust gases in the SCR.

At high temperatures, the rate of heat transfer from wall to droplet is very high, which makes the increase in evaporation rate. This will makes better environment for uniform mixing and occurrence of thermolysis reaction. The comparison of spray for 333K and 573K is shown in figure 6.10.

At this temperature, the urea decomposes into iso-cynaic acid and ammonia. Curly and bouncing spray condition is developed due to the lifting and squeezing of urea spray droplets at this high temperature. During the subsequent spray injection, many of the droplets gets mixed with the gases. Therefore, the number of droplets for uninterrupted injection during impingement declines resulting in the reduction of wall wetting. Due to the high temperature, the evaporation rate in the droplets increases and both axial and radial distances for rebounding droplets in the spray decreases. This will led to better and uniform mixing for SCR reductant with the exhaust gases.

a) b)

Figure 6. 10 Comparison of Spray pattern at a specific time a) 333K and b) 573K

6.7 Effect of Sauter Mean Diameter

The Sauter mean diameter (SMD) is an average of different particle sizes and it is defined as the diameter of a sphere that has same volume to surface area ratio as a particle of interest.

Both the wall temperature and the surroundings temperature are used for calculating the SMD. The development and the breakup of spray droplet had been greatly influenced by the temperature. Both the viscosity and surface tension of spray droplets decreases with increase in temperature, thus the SMD of droplets decreases.

Since, the small droplets evaporates more rapidly, which results in forming more numbers of active elements. This leads to uniform mixing of SCR reductants with exhaust gases and hence reduction in deposits formation.

The SMD of droplets is generally of 50 to 60 microns at temperatures below 513K. From simulations we finds that SMD of droplets has very small fluctuations at wall temperatures less than 513K. This will leads to incomplete evaporation and hence, more solid deposits are formed.

At higher temperatures near to 573K, the droplet size is very small ranging from 35 microns to 40 microns. This leads to faster evaporation of these small droplets, hence there is a decrease in wall wetting and lesser solid deposits are achieved.

The beginning of breakup of droplet is affected by high temperatures. At temperatures of 513K and 573K, droplet breakup begun much earlier than at other temperatures. This will provides large time for mixing and evaporation of droplet.

6.8 Formation of Wall Film

The formation of wall film provides an information of both undesired urea deposits and urea distribution. When the urea is impinged on a hot surface of wall, liquid film is developed. Due to the direct impingement, local cooling occurs, which indirectly dropped the impingement spot temperature rapidly. When the rate of injecting the urea is very high, the temperature can be dropped below the boiling point of water and droplet vaporization is incomplete. The relative velocity of droplets w.r.t. wall surface makes the droplet shattering and hence, minimizing the formation of deposits.

The high impact velocity enhances the droplet shattering and reduces the formation of wall thickness. The high impact velocity can be attained by increasing the injection pressure. At high temperature, we see a reduction in wall film and wall surface cooling.

The wall film formation gets affected by the wall temperature. The wall film thickness behaves as initiating element in formation of solid deposits. So, lower wall temperature is risky for even operations without the formation of deposits.

6.9 Evaporation Tendency of UWS

For investigating the evaporation tendency as a function of time, the rate for urea injection is taken to be 2 g/s. The temperature variations at the wall was from 333K to 573K. The SMD of the spray droplets ranges from 15 μm to 65 μm. Urea fraction in gaseous phase at 0mm and 30mm from injection point is shown in figure 6.11. Spray to wall interaction can be found out by droplet impingement. Quick evaporation of droplet is required for declining the solid deposits. This quick evaporation can be achieved by spraying finer and smaller droplets (this will evaporates faster) or by high wall temperature. From simulation results, we find that the rate of evaporation is not that high till 513K but increased rapidly at 573K. This will reduces the urea deposits.

The droplet size gets smaller with continuous UWS droplets breakup. The size ranges from 10 to 90 microns diameter. But most of the parts ranged from 20 to 75 μm.

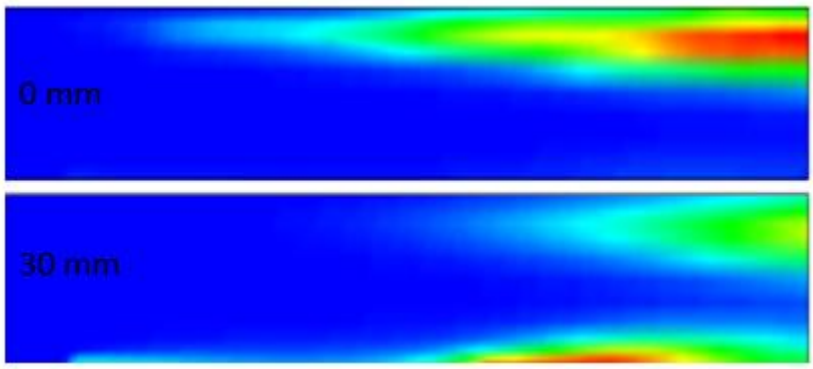

Figure 6. 11 Urea fraction in gaseous phase at 0mm and 30mm from the injection point

CHAPTER 7

CONCLUSION & FUTURE SCOPE

7.1 CONCLUSIONS

The urea water solution impingement on a heated wall was investigated for an SCR system using Ansys 2019R2. Different parameters such as uniformity index and pressure loss were analysed using transient and steady state flow simulations, effect of mass flow rate of exhaust and inlet cone length were studied, effect of turbulent and swirling flow was investigated, also the different geometries of injector with straight and ring type geometries was simulated. During these all activities we needs to find out several other parameters such as wall impingement of spray, wall film formation, size distributions of the urea droplets along with its evaporation rates.

Following conclusions were made from this study:

1. After the spray impingement on the wall, the major parameter that affects the UWS spray is the wall temperature. During higher wall temperatures, the radial projection of spray is larger and there is small axial length. This results in lesser urea deposition due to the effective mixing and proper evaporation at high temperatures.
2. The wall temperature affects inversely to the development of wall film, means at higher temperatures, the wall film thickness is small.
3. The calculated Staunter mean diameter of the droplet is small at high wall temperatures and results in complete evaporation in case of small droplets.
4. The rate of evaporation at lower wall temperatures is quite slower as compared to higher wall temperature due to the higher droplets sizes along with the lesser radial projection of the spray at the lower wall temperature.

Depending upon the simulation results, the influential behaviour of UWS spray and the different parameters in the formation of urea deposition was investigated. It is found that for the reduction in urea deposits, there is a need to increase the rate of evaporation for the droplet at lower wall temperature. For this, the injecting pressure of the spray is either fluctuated and/or dispense the urea spray in larger area. This will optimizes the wall impingement of UWS and lowers the urea deposits.

7.2 FUTURE SCOPE

From this point, there is a need of further research in the direction of characteristics of diesel engines emissions containing Urea-SCR system. The distribution of temperature of aqueous UWS due to the exhaust back-pressure and its impact on the flow rate of device is also required to find out. Along with this the temperature distribution under the different catalyst loading capacity of ammonia requires more briefings. In addition, the effect of dynamic distribution of exhaust gases pressure at the emissions for UWS-SCR system in different environmental conditions including at high terrains, plateau conditions, even at seas and river shores etc. requires more study.

The factor that plays a significant role in disturbing the reaction in the SCR is the temperature. The increase in temperature may cause declination in the NOx conversion. All the model that are referred in this thesis are made with certain assumptions. In the actual system, the heat losses may vary and might be much more than that in simulations. Thus, simulations can also be done while taking care of other heat losses in the UWS-SCR system.

Also, a care for reduction of correlation among different parameters should also be done as one of the parameter may affects the other due to correlation.

References

[1] Rentar Environmental Solutions, September 2018, What are Hydrocarbons and What Hydrocarbons are in Diesel?, "http://rentar.com/hydrocarbons-hydrocarbons-diesel".

[2] Baukal C., (2005) "Everything you need to know about NOx: Controlling and minimizing pollutant emissions is critical for meeting air quality regulations", Pollution control, Metal finishing 103 (11) Page: 18-24.

[3] United States Environmental Protection Agency, September,2018, "http://www.epa.gov/air/nitrogenoxides".

[4] Samarins.com, December,19,2018, How Exhaust Gas Recirculation (EGR) system works, "https://www.samarins.com/glossary/egr-system.html"

[5] Dennis A., Garner C., Taylor D., (1999), "The Effect of EGR on Diesel Engine Wear In-Cylinder Diesel Particulate and NOx Control", SAE 1999-01-0839,

[6] Dagel J., (2002), Diesel Engine and Fuel system Repair, 5th Edition, "Diesel Engine and Fuel System Repair", ISBN 0130929816, Page: 201-202.

[7] Bennett S., (2004), "Medium/Heavy Duty Truck Engines, Fuel & Computerized Management Systems", 2nd Edition, ISBN 1-4018-1499-9. Page: 206.

[8] Leavitt, Wendy, 01/Jul/2008, SCR or EGR?, "https://www.fleetowner.com/management/feature/scr_egr_0701".

[9] Russell A., Epling W.S. (2011), "Diesel Oxidation Catalysts", Cat. Rev.Sci. Eng., 53(4), Page: 337-423.

[10] Autoevolution, How diesel particular particulate works, 8,Jan,2015, https://www.autoevolution.com/news/how-the-diesel-particulatefilter-works-90866.html#agal_0

[11] Kim J.H. et al. (2010), "NO_2-Assisted Soot Regeneration Behavior in a Diesel Particulate Filter with Heavy-Duty Diesel Exhaust Gases", Numerical Heat Transfer Part A Vol.58 No.9 Page: 725–739, Chonbuk National University, Korea.

[12] Sturgess, S., DPF Maintenance ,January 2010, Aftermarket, HDT Trucking Info

[13] Ramon Gracia Gonzalez, After-treatment systems DPF & DOC, December 2018, http://www.drawfolio.com/portfolios/ramongarciagonzalez/picture/50224

[14] Ambs J.L., B.T. McClure, (1993), "The Influence of Oxidation Catalysts on NO_2 in Diesel Exhaust", SAE Technical Paper 932494.

[15] Horan H. (2015), "Eaton aftertreatment System (EAS) for On-Highway Vehicles", 12th Diesel Engine Efficiency and Emissions.

[16] Miller A., Matthey J. (2015), “SCR and advanced ammonia slip Catalyst” Emission Control technologies.

[17] Autoconvertors, Biloxi, September,2018, “https://www.autoconverterrecyclers.com/selective-catalytic-reduction”

[18] Ciardelli C., Nova I., Tronconi E., Chatterjee D., Burkhardt T., and Weibel M. (2007), “NH_3 SCR of NOx for diesel exhaust aftertreatment: role of NO_2 in catalytic mechanism, unsteady kinetics and monolith converter modelling”, Chemical Engineering Science 69, Page: 5001–5006.

[19] Ciardelli C., Nova I., Tronconi E., Chatterjee D., Konrad B.B., Weibel M., and Krutzsch B., (2007), “Reactivity of NO/NO_2-NH_3 SCR system for diesel exhaust aftertreatment: Identification of the reaction network as a function of temperature and NO_2 feed content”, Applied Catalysis B: Environmental 70, Page: 80–90.

[20] Koebel M., Elsener M., and Kleemann M. (2000), “Urea-SCR: A promising technique to reduce NOx emissions from automotive diesel engines”, Catalysis today 59, Page: 335–345.

[21] Schuler A., Votsmeier M., Kiwic P., Gieshoff J., Hautpmann W. ,Drochner A., and Vogel H. (2009), “NH_3-SCR on Fe Zeolite catalysts - from model setup to NH_3 dosing”, Chemical Engineering Journal 154, Page: 333–340.

[22] Willems F.,Cloudt R., Eijnden E., Genderen M., Verbeek R., Jager B., Boomsma W., and Heuvel I. (2007), “Is closed-loop SCR control required to meet future emission targets?”, Tech. report, SAE International.

[23] Strom H., Lundstr¨om A., and Andersson B. (2009), “Choice of urea-spray models in CFD simulations of Urea-SCR systems”, Chemical Engineering Journal 150, Page: 69–82.

[24] Birkhold F., Meingast U., Wassermann P., and Deutschmann O., (2007), “Modeling and simulation of the injection of urea-water solution for automotive SCR denox-systems”, Applied Catalysis B: Environmental 70, Page: 119–127.

[25] Birkhold F., et al. (2006), “Analysis of the Injection of Urea-Water-Solution for Automotive SCR DeNOx-Systems: Modeling of Two-Phase Flow and Spray/Wall-Interaction”, SAE International.

[26] Abramzon B., Sirignano, W. A. (1989), “Droplet vaporization model for spray combustion calculations”, International journal of heat and mass transfer, 32(9), Page: 1605-1618.

[27] Alekhya R., Rao V.S. (2017), “Conjugate Heat Transfer Analysis of Exhaust After-Treatment Systems”, International Journal of Research and Innovation (IJRI) 4.1 Page: 585-594.

[28] Birkhold F., Meingast U., Wassermann P.,Deutschmann O. (2007), “Modeling and simulation of the injection of Urea-water-solution for automotive SCR DeNOx-systems” Applied Catalysis B: Environmental 70, Page: 119–127

[29] Damm M.A., Sauerborn M.A., Fend T., Herrmann U. (2017), “Optimisation of a Urea Selective Catalytic Reduction System with a Coated Ceramic Mixing Element”, Journal of Ceramic Science & Technology; 08 [0 1], Page: 19-24.

[30] Diao C. , Guo X., Li J., (2018), “Research on Urea Jet Pump Performance Characteristics using the Optimized NOx Removal Equipment in Diesel Engine Aerosol and Air Quality Research”, 18: Page: 1886–1900.

[31] Dixit, M., Sundaram, V., and Sathish Kumar, S. (2016), “A Novel Approach for Flow Simulation and Back Pressure Prediction of Cold End Exhaust System”, SAE Technical Paper.

[32] Hüthwohl G., Dolenec S. (2011), “A new Approach in AdBlue Dosing to Improve Performance and Durability of SCR Systems for the Use in Passenger Cars up to Heavy Duty Vehicles”, SAE 2011-01-209.5

[33] Jeong S.J., Kim, W.S. (2003), “A study on the optimal monolith combination for improving flow uniformity and warm-up performance of an auto-catalyst”, Chemical Engineering and Processing, 42, Page: 879 – 895.

[34] Jeong S.J., Lee S.J., Kim W.S., Lee C.B. (2005), “Simulation on the Optimum Shape and Location of Urea Injector for Urea-SCR System of Heavy-duty Diesel Engine to Prevent NH_3 Slip”; SAE 100, SAE Technical Paper Series, 2005-01-3886.

[35] Kim T., Choi B. (2017), “Numerical analysis of the melting characteristics of a frozen Urea-Water Solution by heat spreaders with a positive temperature coefficient heater”, Applied Thermal Engineering 119, Page: 275–282.

[36] Konstandopoulos A.G., Kostoglou M., Beatrice C., Blasio G.D., Imren A., Denbratt I., (2015), “Impact of Combination of EGR, SCR, and DPF Technologies for the Low-Emission Rail Diesel Engines”, Emiss. Control Sci. Technol. 1, Page: 213–225.

[37] Michelin, J., Nappez, P., Guilbaud, F., Hinterberger, C. et al. (2015), “Advanced Close Coupled SCR Compact Mixer Architecture”, SAE Technical Paper 2015-01-1020.

[38] Park T., Lee I., Choi G. et al. (2014), “Effect of static mixer geometry on flow mixing and pressure drop in marine SCR applications”, Int. J. Nav. Archit. Ocean Eng 6, Page: 27-38.

[39] Peters A., Freising, Marko Buder, Ingolstadt, Gerdon S., Hayna, Kohrs S., Neustadt et al (2015), “Static Mixer for an Exhaust Gas System of an Internal Combustion Engine Driven Vehicle, in particular Motor Vehicle”, Patent no: US 9,003,771 B2.

[40] Beale, Jennifer & Reitz, Rolf. (1999), Modeling spray atomization with the Kelvin-Helmholtz/Rayleigh-Taylor hybrid model, Atomization and Sprays, 9, Page 623-650.

[41] Sala R., Bielaczyc B., Brzezanski M. (2017), “Concept of Vaporized Urea Dosing in Selective Catalytic Reduction”, Catalysts.

[42] Salanta G., Zheng G., Kotrba A. and Rampazzo R., Bergantim L. (2010), “Optimization of a Urea SCR System for On-Highway Truck Applications”, SAE International 2010-01-1938.

[43] Seo J. (2011), “Aftertreatment Package Design for SCR Performance Optimization” SAE International 2011-01-1135.

[44] Sharma S., Fadnavis J., Khot A. (2017), “Empirical Model to Predict Melt Volume for different range of Diesel Exhaust Fluid Tank Volumes used in Selective Catalytic Reduction Systems”, Applied Thermal Engineering.

[45] Sheong H.J. (2012), “Selective Catalytic Reduction (SCR) of NO by NH_3 in a fixed bed reactor”, MS Dissertation, The Pennsylvania State University, EGEE 520.

[46] Way P., Viswanathan K., Preethi P., Gilb A., et al. (2009), “SCR Performance Optimization through Advancements in Aftertreatment Packaging”, SAE International 2009-01-0633

[47] Wiesche S. (2007), “Numerical heat transfer and thermal engineering of AdBlue (SCR) tanks for combustion engine emission reduction”, Applied Thermal Engineering 27, Page: 1790–1798

[48] Wu B., Tang G., Chen X., Zhou C.Q., Colella C.P., Okosun T. (2014), “Optimization of an Urea Decomposition Chamber Using CFD and VR”, Applied Thermal Engineering.

[49] Wu, Y., Liang, X., Shu, G., Shen, B. et al. (2017), “Simulation Research of the Structural Downsizing of SCR Reactor”, SAE Technical Paper 2017-01-2387.

[50] Zheng, G., Wang, F., Zhang, S., Zhang, J. et al. (2014), “Development of Compact SCR Systems with Closely Coupled Injector Configurations”, SAE Technical Paper 2014-01-1546.

[51] Twigg M.V. (2007), “Progress and future challenges in controlling automotive exhaust gas emissions”, Applied Catalysis B: Environmental 70, Page: 2–15.

[52] Zhang X., Romzek M., and Morgan C., (2006) “3-D Numerical Study of Mixing Characteristics of NH_3 in Front of SCR,” SAE International.

[53] Chen M. and William S., (2005) “Modelling and Optimization of SCR-Exhaust After-treatment Systems,” SAE Technical Paper 2005-01-0969.

Himanshu

ORIGINALITY REPORT

13%	5%	7%	6%
SIMILARITY INDEX	INTERNET SOURCES	PUBLICATIONS	STUDENT PAPERS

PRIMARY SOURCES

1	www.dieselnet.com Internet Source	2%
2	Xiaogang Zhang, Martin Romzek. "Computational Fluid Dynamics (CFD) Applications in Vehicle Exhaust System", SAE International, 2008 Publication	2%
3	publications.lib.chalmers.se Internet Source	1%
4	www.nett.ca Internet Source	1%
5	Felix Birkhold, Ulrich Meingast, Peter Wassermann, Olaf Deutschmann. "Modeling and simulation of the injection of urea-water-solution for automotive SCR DeNOx-systems", Applied Catalysis B: Environmental, 2007 Publication	<1%
6	Gan, Xubo, Dongwei Yao, Feng Wu, Jiawei Dai, Lai Wei, and Xingwen Li. "Modeling and simulation of urea-water-solution droplet	<1%

evaporation and thermolysis processes for SCR systems", Chinese Journal of Chemical Engineering, 2016.
Publication

7	papers.sae.org Internet Source	<1%
8	Stefan aus der Wiesche. "Numerical heat transfer and thermal engineering of AdBlue (SCR) tanks for combustion engine emission reduction", Applied Thermal Engineering, 2007 Publication	<1%
9	Guanyu Zheng, Fengshuang Wang, Suying Zhang, Jianhua Zhang, Jianzhong Tao, Zhiguo Zhao, Jianqing Fan. "Development of Compact SCR Systems with Closely Coupled Injector Configurations", SAE International, 2014 Publication	<1%
10	Chunyan Diao, Xingmeng Guo, Jianfeng Li. "Research on Urea Jet Pump Performance Characteristics using the Optimized NOx Removal Equipment in Diesel Engine", Aerosol and Air Quality Research, 2018 Publication	<1%
11	Joel Michelin, Philippe Nappez, Frederic Guilbaud, Christof Hinterberger et al. "Advanced Close Coupled SCR Compact Mixer Architecture", SAE International, 2015	<1%

Publication

12	Xubo Gan, Dongwei Yao, Feng Wu, Jiawei Dai, Lai Wei, Xingwen Li. "Modeling and simulation of urea-water-solution droplet evaporation and thermolysis processes for SCR systems", Chinese Journal of Chemical Engineering, 2016 Publication	<1%
13	www.xaam.in Internet Source	<1%
14	Submitted to University of Limerick Student Paper	<1%
15	www.fxsolver.com Internet Source	<1%
16	Submitted to Birzeit University Main Library Student Paper	<1%
17	Submitted to Thapar University, Patiala Student Paper	<1%
18	Jungmin Seo. "Aftertreatment Package Design for SCR Performance Optimization", SAE International, 2011 Publication	<1%
19	ABRAMZON, B., and W. SIRIGNANO. "Droplet vaporization model for spray combustion calculations", 26th Aerospace Sciences Meeting, 1988. Publication	<1%

20	Kamel Ghali, Nesreen Ghaddar, Mohamad Salam. "Radiant Domestic Combustion Stove System: Experimental and Simulated Study of Energy Use and Thermal Comfort", International Journal of Green Energy, 2005 Publication	<1%
21	Submitted to University of Warwick Student Paper	<1%
22	"Urea-SCR Technology for deNOx After Treatment of Diesel Exhausts", Springer Science and Business Media LLC, 2014 Publication	<1%
23	Submitted to Staffordshire University Student Paper	<1%
24	Taewook Kim, Byungchul Choi, Seunghun Jung. "Numerical analysis of the melting characteristics of a frozen urea-water solution by heat spreaders with a positive temperature coefficient heater", Applied Thermal Engineering, 2017 Publication	<1%
25	Submitted to University of Hertfordshire Student Paper	<1%
26	Submitted to BITS, Pilani-Dubai Student Paper	<1%

27	Manish Dixit, V Sundaram, S. Sathish Kumar. "A Novel Approach for Flow Simulation and Back Pressure Prediction of Cold End Exhaust System", SAE International, 2016 Publication	<1%
28	Xiaogang Zhang, Martin Romzek, Chris Morgan. "3-D Numerical Study of Mixing Characteristics of NH3 in Front of SCR", SAE International, 2006 Publication	<1%
29	Jakov Baleta, Matija Martinjak, Milan Vujanović, Klaus Pachler, Jin Wang, Neven Duić. "Numerical analysis of ammonia homogenization for selective catalytic reduction application", Journal of Environmental Management, 2017 Publication	<1%
30	Taewha Park, Yonmo Sung, Taekyung Kim, Inwon Lee, Gyungmin Choi, Duckjool Kim. "Effect of static mixer geometry on flow mixing and pressure drop in marine SCR applications", International Journal of Naval Architecture and Ocean Engineering, 2014 Publication	<1%
31	MY Raghu, Prashant Sharma. "Evaluation of Performance of DPF Cell Structure for Soot Loading, Regeneration and Pressure Drop	<1%

Using CFD Simulation", SAE International, 2017
Publication

32	"Emission Control", University/Engineering, 2010-09-16 Publication	<1%
33	Submitted to University of Leeds Student Paper	<1%
34	Submitted to Coventry University Student Paper	<1%
35	Submitted to Middle East Technical University Student Paper	<1%
36	Athanasios G. Konstandopoulos, Margaritis Kostoglou, Carlo Beatrice, Gabriele Di Blasio, Abdurrahman Imren, Ingemar Denbratt. "Impact of Combination of EGR, SCR, and DPF Technologies for the Low-Emission Rail Diesel Engines", Emission Control Science and Technology, 2015 Publication	<1%
37	Ramesha Chandrappa, Umesh Chandra Kulshrestha. "Chapter 4 Fundamentals of Treatment, and Process Design for Air Pollution Control", Springer Science and Business Media LLC, 2016 Publication	<1%
38	Submitted to Jawaharlal Nehru Technological	

	University Anantapur Student Paper	<1%
39	eur-lex.europa.eu Internet Source	<1%
40	iasbyheart.com Internet Source	<1%
41	Submitted to Texas State Technical College Student Paper	<1%
42	d-nb.info Internet Source	<1%
43	Submitted to Rajarambapu Institute of Technology Student Paper	<1%
44	Submitted to Gyeongsang National University Student Paper	<1%
45	Submitted to University of Sheffield Student Paper	<1%
46	A. Berlemont, M.S. Grancher, G. Gouesbet. "Heat and mass transfer coupling between vaporizing droplets and turbulence using a lagrangian approach", International Journal of Heat and Mass Transfer, 1995 Publication	<1%
47	Soo-Jin Jeong, Woo-Seung Kim. "A study on the optimal monolith combination for improving	<1%

	flow uniformity and warm-up performance of an auto-catalyst", Chemical Engineering and Processing: Process Intensification, 2003 Publication	
48	Submitted to University College London Student Paper	<1%
49	environment.gov.au Internet Source	<1%
50	Submitted to Korea University Student Paper	<1%
51	Submitted to University of Strathclyde Student Paper	<1%
52	Submitted to Visvesvaraya Technological University Student Paper	<1%
53	Submitted to Fanshawe College of Applied Arts and Technology Student Paper	<1%
54	Xiaogang Zhang, Martin Romzek. "3-D Numerical Study of Flow Mixing in Front of SCR for Different Injection Systems", SAE International, 2007 Publication	<1%
55	Submitted to UNITEC Institute of Technology Student Paper	<1%

56	Submitted to King Fahd University for Petroleum and Minerals Student Paper	<1%
57	Abramzon, B.. "Droplet vaporization model for spray combustion calculations", International Journal of Heat and Mass Transfer, 198909 Publication	<1%
58	Submitted to The University of Manchester Student Paper	<1%
59	Yong Yi. "Development of a 3D Numerical Model for Predicting Spray, Urea Decomposition and Mixing in SCR Systems", SAE International, 2007 Publication	<1%
60	www.tritonia.fi Internet Source	<1%
61	Submitted to Kingston University Student Paper	<1%
62	Submitted to Liverpool John Moores University Student Paper	<1%
63	Submitted to Cranfield University Student Paper	<1%
64	V. Praveena, M. Leenus Jesu Martin. "A review on various after treatment techniques to reduce NOx emissions in a CI engine", Journal of the	<1%

Energy Institute, 2017

Publication

Exclude quotes	On	Exclude matches	< 8 words
Exclude bibliography	On		